Provided for non-commercial research and education use.
Not for reproduction, distribution or commercial use.

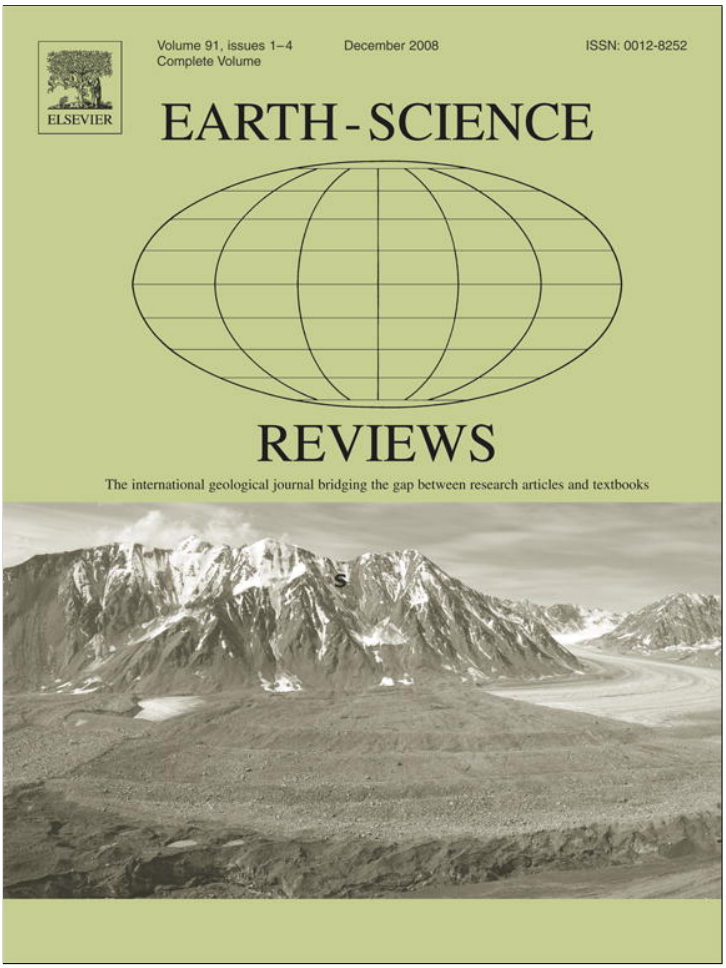


This article appeared in a journal published by Elsevier. The attached copy is furnished to the author for internal non-commercial research and education use, including for instruction at the authors institution and sharing with colleagues.

Other uses, including reproduction and distribution, or selling or licensing copies, or posting to personal, institutional or third party websites are prohibited.

In most cases authors are permitted to post their version of the article (e.g. in Word or Tex form) to their personal website or institutional repository. Authors requiring further information regarding Elsevier's archiving and manuscript policies are encouraged to visit:

http://www.elsevier.com/copyright

Author's personal copy

Earth-Science Reviews 91 (2008) 1–26

Contents lists available at ScienceDirect

Earth-Science Reviews

journal homepage: www.elsevier.com/locate/earscirev

# Passive margins through earth history

Dwight C. Bradley

*U.S. Geological Survey, 4200 University Drive, Anchorage, Alaska 99508, USA*

ARTICLE INFO

*Article history:*
Received 7 September 2007
Accepted 4 August 2008
Available online 22 August 2008

*Keywords:*
passive margin
plate tectonics
plate velocity
arc–continent collision
foreland basin
supercontinent

ABSTRACT

Passive margins have existed somewhere on Earth almost continually since 2740 Ma. They were abundant at 1900–1890, 610–520, and 150–0 Ma, scarce at ca. 2445–2300, 1600–1000, and 300–275 Ma, and absent before ca. 3000 Ma and at 1740–1600. The fluctuations in abundance of passive margins track the first-order fluctuations of the independently derived seawater $^{87}Sr/^{86}Sr$ secular curve, and the compilation thus appears to be robust. The 76 ancient passive margins for which lifespans could be measured have a mean lifespan of 181 m.y. The world-record holder, with a lifespan of 590 m.y., is the Mesoproterozoic eastern margin of the Siberian craton. Subdivided into natural age groups, mean lifespans are 186 m.y. for the Archean to Paleoproterozoic, 394 m.y. for the Mesoproterozoic, 180 m.y. for the Neoproterozoic, 137 m.y. for the Cambrian to Carboniferous, and 130 m.y. for the Permian to Neogene. The present-day passive margins, which are not yet finished with their lifespans, have a mean age of 104 m.y. and a maximum age of 180 m.y. On average, Precambrian margins thus had longer, not shorter, lifespans than Phanerozoic ones—and this remains the case even discounting all post-300 Ma margins, most of which have time left. Longer lifespans deeper in the past is at odds with the widely held notion that the tempo of plate tectonics was faster in the Precambrian than at present. It is entirely consistent, however, with recent modeling by Korenaga [Korenaga, J., 2004. Archean geodynamics and thermal evolution of Earth. Archean Geodynamics and Environments, AGU Geophysical Monograph Series 164, 7–32], which showed that plate tectonics was more sluggish in the Precambrian. The abundance of passive margins clearly tracks the assembly, tenure, and breakup of Pangea. Earlier parts of the hypothesized supercontinent cycle, however, are only partly consistent with the documented abundance of passive margins. The passive-margin record is not obviously consistent with the proposed breakup of Nuna (Columbia), the assembly of Rodinia, or the assembly or breakup of the putative Pannotia. An alternative model is put forth involving (a) formation of two or more supercratons during the late Paleoproterozoic, (b) a Mesoproterozoic interval dominated by lateral accretion of arcs rather than by continental breakup and dispersal, (c) wholesale collision to form Rodinia by the end of the Mesoproterozoic, and (d) staged breakup of Rodinia through much of the Neoproterozoic.

Published by Elsevier B.V.

**Contents**

1. Introduction . . . 2
2. Methods . . . 2
   2.1. Definitions . . . 2
   2.2. Criteria for recognition of ancient passive margins . . . 3
   2.3. Fates of passive margins . . . 3
   2.4. Determining the start date and end date . . . 3
   2.5. Census methods, disclaimers, and error estimates . . . 5
3. Modern passive margins . . . 7
4. Ancient passive margins . . . 7
   4.1. Present-day collision between Australia and the Banda forearc . . . 7
   4.2. Cambrian–Ordovician Appalachian margin of Laurentia . . . 10
   4.3. Verkhoyansk (eastern) margin of Siberia . . . 14
   4.4. Western margin of Kaapvaal craton . . . 16
5. Distribution of passive margins through time . . . 16
6. Lifespans of passive margins through time and implications for the tempo of plate tectonics . . . 18

*E-mail address:* dbradley@usgs.gov.

0012-8252/$ – see front matter. Published by Elsevier B.V.
doi:10.1016/j.earscirev.2008.08.001

Author's personal copy



7. Secular changes in the geology of arc–passive margin collision . . . 19
7.1. High-pressure, low-temperature metamorphism . . . 19
7.2. Foredeep magmatism . . . 20
8. Comparisons with postulated supercontinents . . . 20
8.1. Pangea . . . 21
8.2. Pannotia . . . 21
8.3. Rodinia . . . 21
8.4. Nuna . . . 22
8.5. Sclavia, Superia, and Vaalbara . . . 22
8.6. Proposed scenario . . . 22
8.7. Implications for continental reconstructions . . . 23
9. Comparisons with other aspects of Earth history . . . 23
9.1. Isotopic composition of seawater strontium . . . 23
9.2. Juvenile crust . . . 23
9.3. Massif anorthosites . . . 23
10. Less common fates of passive margins . . . 24
10.1. Re-rifting . . . 24
10.2. Conversion to a convergent margin . . . 24
11. Summary . . . 24
Acknowledgments . . . 25
References . . . 25

## 1. Introduction

Passive margins are among the most common of the Earth's first-order tectonic features. The present-day passive margins have an aggregate length of 105,000 km, even longer than the spreading ridges (65,000 km) or the convergent plate boundaries (53,000 km). Since the Neoarchean, passive margins have been key players in Wilson Cycles (Burke et al., 1976). Sedimentary successions formed during the rift, drift, and collision stages of passive-margin evolution are major repositories of the stratigraphic record. These strata contain a substantial fraction of the world's hydrocarbon resources (Mann et al., 2003), carbonate-hosted lead–zinc deposits (Leach et al., 2001), and phosphorite deposits (Cook and McElhinny, 1979).

It is surprising, then, that the ancient passive margins have never been systematically studied as a group. When did the first one form? Has their distribution through Earth history been roughly constant or irregular? What is the average duration, or "lifespan", of a passive margin and how has this value changed over time, in response to the decline in Earth's radiogenic heat production? What is the longest-lived passive margin on record? The present study addresses these questions through a survey of the regional geologic literature. In assessing the history of each candidate margin, the goals were: (1) to document the tectonic evolution of the margin, (2) to establish the timing of the rift-drift transition, (3) to establish the timing of the passive margin to foreland-basin transition (except for those rare margins that met another fate), and (4) to identify critical targets for geochronological study. For context, the ages of all the present-day passive margins–those that have yet to complete their Wilson Cycles–were also compiled.

An early synthesis of passive margins was published, in abstract only, by Burke et al. (1984). They estimated the lifespans of 25 mostly Phanerozoic passive margins, and debunked what at the time was a popular idea: that passive margins commonly convert into Andean-type margins by growing old and failing in compression. In a study of supercontinent behavior, Condie (2002) tabulated approximate ages of 38 rifting events and 39 subsequent collisions over the past 1400 Ma. His rifting estimates, however, were based on conflated data from pairs of supposedly conjugate margins (*e.g.*, Laurentia–Kalahari). Accordingly, it is impossible to parse breakup ages (rift-drift transitions) for individual margins from Condie's (2002) data table. The focus of the present study was to document both the abundance of passive margins and their individual lifespans as a function of time. Preliminary accounts of the present study were presented by Bradley in 2005, when the count stood at 50 ancient margins, and in 2007, when the number had reached 63. The present paper covers 85 ancient margins. There remain many more to be mined from the literature, particularly in the Tethyan realm, but the 85 margins are sufficient to reveal first-order trends.

## 2. Methods

### 2.1. Definitions

The term *passive margin* is a synonym for the bulkier *Atlantic-type margin*, *trailing-edge margin*, *rifted margin*, or *divergent margin*. A passive margin is one formed by rifting followed by seafloor spreading, so that the resulting plate consists of both continental and oceanic lithosphere, welded across an igneous contact. The distinction between "lower-plate" and "upper-plate" (or volcanic versus non-volcanic) subtypes of passive margins (*e.g.*, Lister et al., 1991) has only been made for a few of the ancient margins in the present compilation. This should be pursued further, as it will help in refining the ages of some rift-drift transitions, as Stampfli et al. (1991) have done for several Tethyan margins. Portions of passive margins that evolved from transform segments of ridge-transform systems (*i.e., sheared passive continental margins* of Scrutton, 1982) are included in the present study. Passive margins formed by backarc extension are a special case. For this study, margins along the continental sides of backarc basins are included (*e.g.*, Chinese margin of the South China Sea), but the volcanic-arc margins of such basins are excluded (The latter would likely be recognized in the rock record as an arc rather than as a passive margin.). Also excluded are any margins that might be more accurately termed *inactive margins*—ones that became "passive" when subduction along a convergent margin stopped. An important distinction in the present compilation is between the modern margins, which face extant ocean basins, and the ancient margins, which occur in orogenic belts.

The entry of a passive margin into a subduction zone is referred to as an *arc–passive margin collision*. In such collisions, it is the forearc and not the magmatic arc that comes into contact with the passive margin; commonly the forearc is a recently formed ophiolite and its syncollisional thrust emplacement is what some workers refer to as *obduction*. For present purposes, it makes little difference whether a collision was of extensional or compressional character, or whether

Author's personal copy



the overriding plate was an oceanic arc or a continental margin—what matters is when collision began. Severely tectonized margins that have been through multiple orogenies are hard to unravel, and this is a particular problem for identification and analysis of Archean and Proterozoic margins. Another challenge is in working out the history of two successive margins that lie one atop the other: the arc that collides to end the first cycle may be carried away at the start of the second cycle.

### 2.2. Criteria for recognition of ancient passive margins

All of the ancient passive margins have been trapped within orogenic belts and are no longer flanked by ocean floor. Nonetheless, many are still readily recognized by the following criteria: (1) they flank cratons or microcontinents; (2) they are underlain by continental basement, which may or may not have a sedimentary cover predating origination of the margin in question; (3) rift basins overlie the basement; (4) rift deposits and basement are together overlain by an immediately younger, seaward-thickening, seaward-deepening miogeoclinal prism; (5) shallow-water deposits of the miogeoclinal prism are (or more commonly, were) flanked by coeval deep-water facies inferred to have been deposited by stretched continental or oceanic lithosphere, and (6) ophiolites and/or arc sequences were later thrust onto platfom deposits, providing evidence that an ocean basin once existed next to the miogeocline. The deep-water facies and ophiolites also aid in the distinction between a passive margin that was involved in collision, and a deformed (inverted) intracratonic basin that was flanked on all sides by continent and never faced a true ocean.

The hallmark of a passive margin is a miogeoclinal prism—a sedimentary wedge that thickens seaward from a feather edge to 15 km or more. Most easily recognized are miogeoclinal prisms that formed at low latitudes and consequently are dominated by carbonate rocks: limestone, dolostone, and metamorphosed equivalents. In contrast, high-latitude miogeoclinal prisms are typified by compositionally mature shallow-marine sandstone, siltstone, and shale. A carbonate platform succession can still be recognized for what it was despite high-grade metamorphism whereas the depositional setting of metamorphosed siliciclastic rocks may not be so easy to unravel.

### 2.3. Fates of passive margins

Each of the ancient passive margins in the present synthesis had one of three fates: (1) collision, (2) re-rifting, or (3) direct conversion to a convergent margin (Fig. 1). Most passive margins since the Neoarchean met the first fate: they formed by rifting, endured for a time, and ultimately collided with an arc (Fig. 2). This paper is mainly concerned with this dominant subset of passive margins; the other fates are briefly discussed in Section 10.

### 2.4. Determining the start date and end date

For modern passive margins, the *start date* (age of initiation) is the age of the oldest magnetic anomaly next to the margin. For ancient passive margins, the equivalent time is approximated by the so-called rift-drift transition—an upward transition from local, fault-controlled rift-type facies (immature clastics, basalt, lacustrine deposits, evaporites) to regionally extensive platformal carbonates (at lower latitudes) or siliciclastics (at high latitudes) (Fig. 2a). In some cases, a breakup unconformity is taken as approximating the rift-drift transition. Tectonic subsidence curves typically show a sharp bend representing a transition from rapid, fault-controlled subsidence to slower, exponential, thermally controlled subsidence; the inflection point approximates the rift-drift transition. Dating the rift-drift transition is more difficult than dating the passive-margin to foreland-basin transition because (1) mafic rocks that typify rift settings are more difficult to date than felsic tuffs and syntectonic granitoids in collisional settings; (2) the onset of seafloor spreading corresponds to a shift in the locus of tectonism to a place where preservation is highly unlikely, (3) rifting before seafloor spreading often lasts many

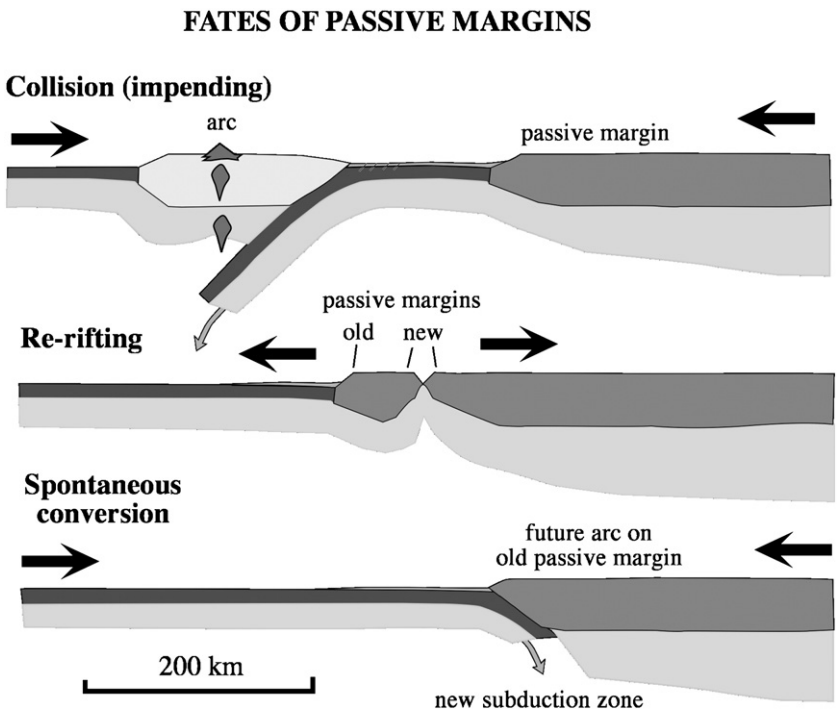


**Fig. 1.** The three common fates of passive margins. (a) Collision between a passive margin and an arc. For the aims of this study, the nature of this arc–whether intraoceanic or continental, and whether extensional or compressional–is not important. (b) Re-rifting of a preexisting passive margin by separation of a ribbon microcontinent. (c) Spontaneous conversion of a passive margin to a convergent margin by initiation of a subduction zone at or near the ocean–continent boundary.

Author's personal copy



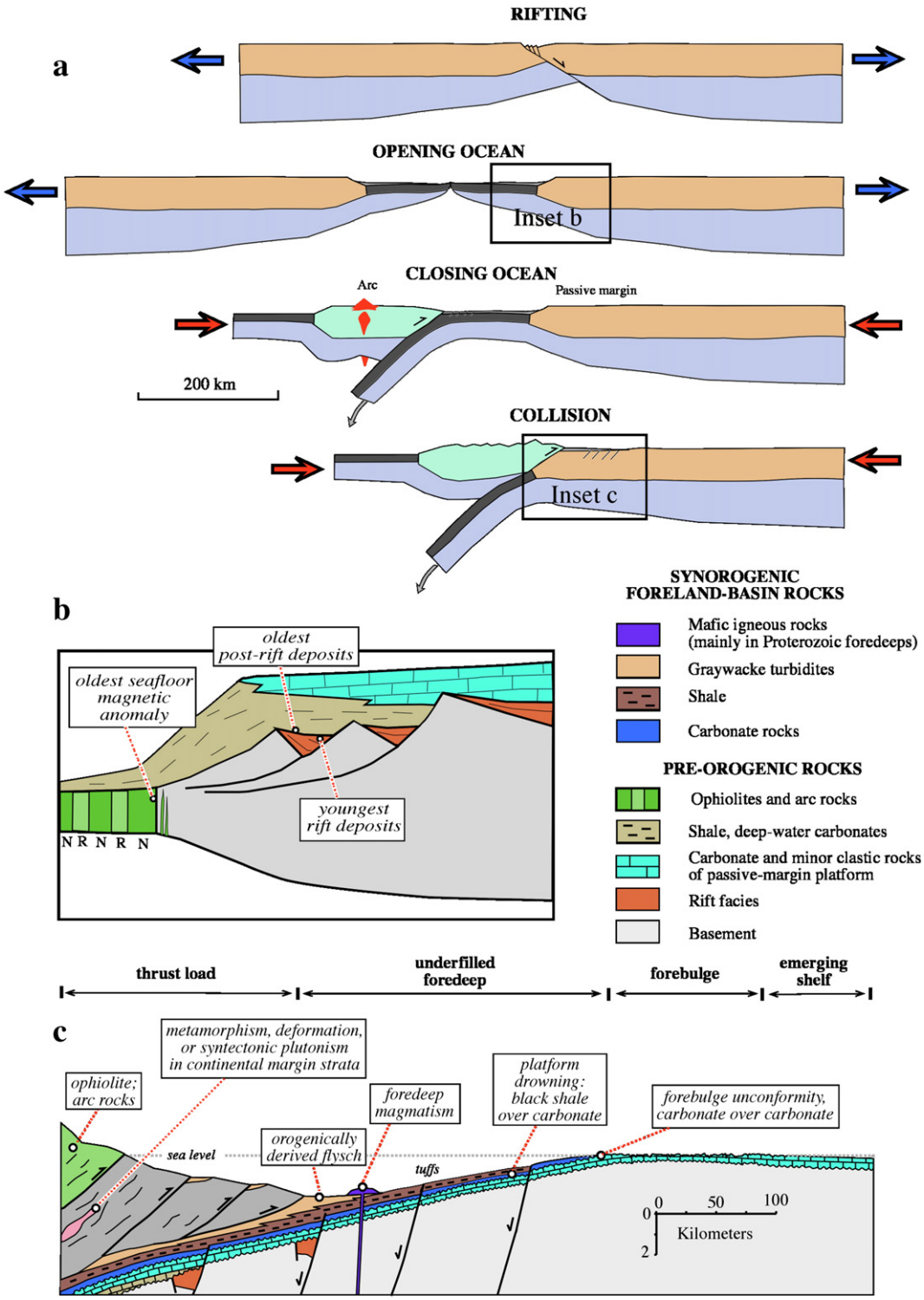


**Fig. 2.** (a) Model of passive-margin evolution showing stages of rifting, seafloor spreading, ocean closure, and collision. (b) Close-up showing criteria for picking the age of the rift-drift transition ("start date" in text). (c) Close-up showing criteria for picking the age of the passive-margin to foreland-basin transition ("end date" in text).

tens or even hundreds of millions of years, so dated rift deposits may not provide very precise age bracketing, and (4) most passive-margin successions lack igneous rocks entirely and thus are not *directly* datable by the most common targets of conventional isotope geochronology. Less direct age constraints on the age of the rift-drift transition are also provided by oceanic rocks in some orogens. When an arc eventually collides with a passive margin, the oldest arc rocks are commonly interpreted to date the onset of subduction. Barring complications, the rift-drift transition at the passive margin should be older still.

For passive margins that ended with collision, the *end date* is defined here as the time when the continent–ocean boundary is subducted, as is happening today just south of Taiwan (Malavieille et al., 2002). The end date can be gleaned from sedimentary rocks in the undeformed foreland, and from sedimentary, igneous, and metamorphic rocks within the orogen (Fig. 2c). The stratigraphic signature

Author's personal copy



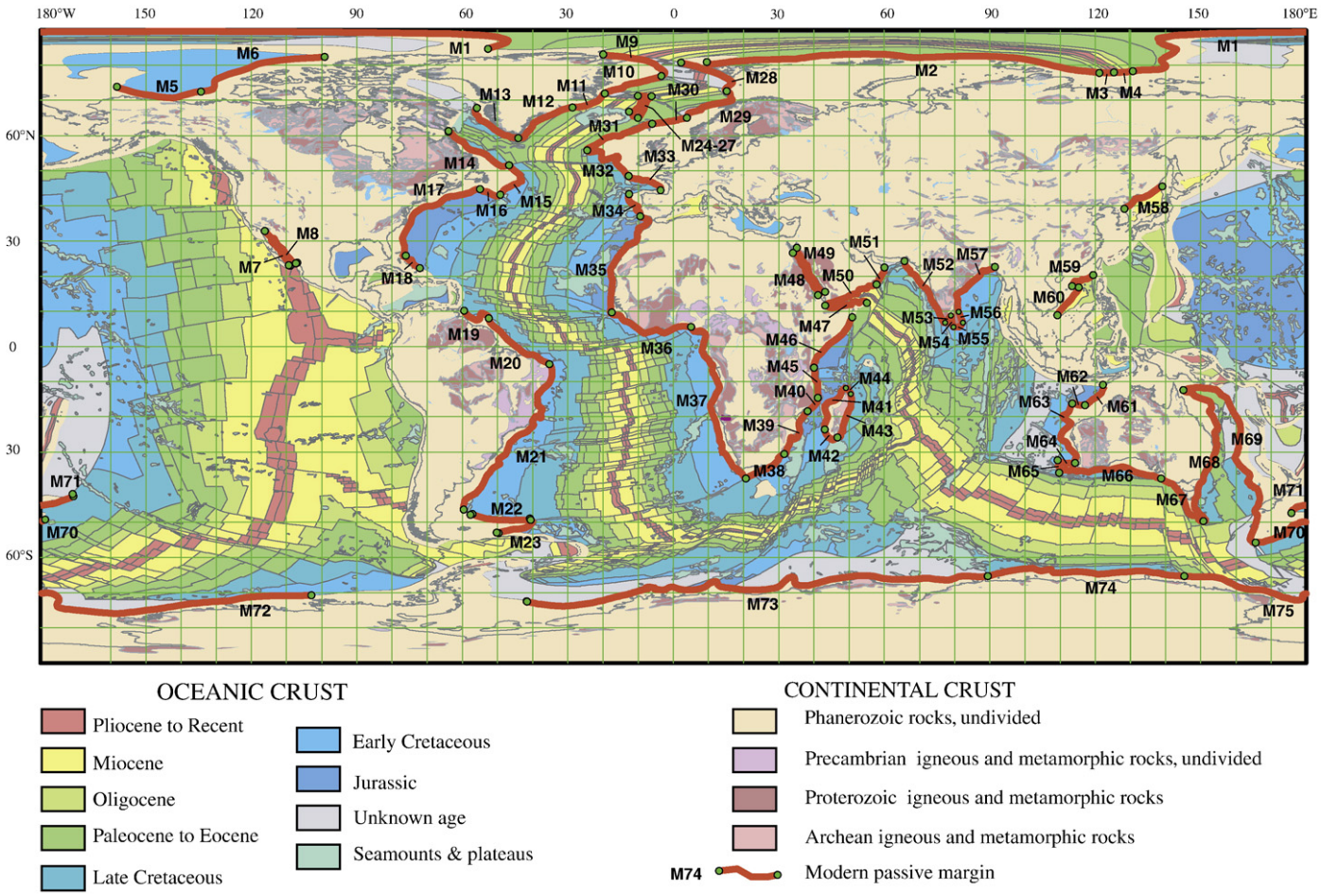


**Fig. 3.** World map showing modern passive margins. Base map from Commission de la Carte Géologique du Monde (2000). Green circles divide margins into age sectors.

of an arc–passive margin collisional foreland is remarkably systematic (*e.g.*, Rowley and Kidd, 1981; Bradley, 1989; Sinclair, 1997) and is described in Section 4.2 on the Appalachian margin. Briefly, the transition from passive margin to foreland basin is recorded by a platform drowning sequence and influx of outboard-derived siliciclastics; many dating opportunities are afforded by fossils and (or) ashfall tuffs. Syncollisional extension of the foreland–a consequence of flexural loading of the passive-margin plate (Bradley and Kidd, 1991)–is common, and in some orogens has been mistaken for rifting at the *start* of the Wilson Cycle. In some cases, the best age control comes from within the orogenic belt itself, as revealed by the age of initial metamorphism of continental-margin rocks or by the age of the oldest syntectonic plutons in the orogenic wedge.

### *2.5. Census methods, disclaimers, and error estimates*

The present compilation includes summaries of 85 passive margins, based almost exclusively on the recent English-language literature. A number of margins were unearthed using the Georef bibliographic database, by means of search criteria such as "Amazonia" plus "passive margin", "Mesoproterozoic" plus "passive margin", and "India" plus "passive margin". Schematic plate reconstructions (*e.g.*, Sengör et al., 1988; Stampfli et al., 1991; Zhao et al., 2002, 2004; Scotese, 2004) provided leads to other margins.

The most severe errors are likely to come from tectonic misinterpretations. Despite the fact that arc–passive margin collisions are the most tractable type of orogeny, every such collision has its controversies and interpretive problems. Even in the thoroughly studied Wopmay and Appalachian orogens, rift and foreland-basin sequences were once mistaken for one another. In working out a margin's lifespan, this kind of mistake would trump all other potential errors. Even when the tectonostratigraphic framework has been correctly interpreted, age control may be poor. Ideally, the rift-drift and passive margin-foreland-basin transitions are tightly bracketed by dated rocks from immediately below and immediately above the crucial boundaries; but in reality, the rock record is not so forthcoming. Uncertainties simply cannot be quantified where one of the key age constraints is a guess. The only kinds of uncertainties that can be quantified are encountered at a more detailed level, such as analytical errors of geochronological ages, biostratigraphic uncertainty of fossil collections, and uncertainties in the calibration of the geologic time scale.[1]

Given the many potential problems, it is fruitless to guess at the numerical error associated with the start date, end date, and lifespan for most margins. Instead, each margin is assigned an overall quality rating on a scale from A to D (best to worst). A margin with a rating of "A" has a robust tectonic interpretation, and both the start date and end date are reasonably well constrained; the estimated lifespan is probably correct within 10 to 20 million years. A quality rating of "B" is given when one key ingredient–start date, end date, or tectonic interpretation–is weak. A passive margin given a rating of "C" is only minimally acceptable for this study: both the tectonic interpretation and the lifespan estimate are debatable. For margins with quality

[1] The recent Gradstein and Ogg (2004) time scale was used here to assign numerical ages to stratigraphically or paleontologically defined events in the Phanerozoic. Where previous workers used an alternative older time scale for this purpose, the numbers have been revised accordingly.

Author's personal copy



**Table 1**
Modern passive margins. For locations, see Fig. 3. See the Appendix for notes that explain some of the more difficult age picks. Adapted from a preliminary compilation by David Rowley

| Number | Margin name | Ocean | Oldest age (Ma) | Youngest age (Ma) | Mean age (Ma) | Length (km) |
|---|---|---|---|---|---|---|
| M1 | Lomonosov Ridge, facing Barents shelf (R edge map) | Arctic | 60 | 58.4 | 59.2 | 1393 |
| M1 | Lomonosov Ridge, facing Barents shelf (L edge map) | Arctic (Eurasian Basin) | 60 | 58.4 | 59.2 | 633 |
| M2 | Europe, N margin (Barents shelf) | Arctic | 58.4 | 15.4 | 36.9 | 2328 |
| M3 | Eurasia, N coast (Lena delta W of Gakkel ridge) | Arctic | 52 | 0 | 26.0 | 109 |
| M4 | Eurasia, N coast (Lena delta E of Gakkel ridge) | Arctic | 52 | 0 | 26.0 | 129 |
| M5 | Alaska, N coast | Arctic (Canada Basin) | 130.2 | 130.2 | 130.2 | 789 |
| M6 | Canada, N coast | Arctic (Canada Basin) | 130.2 | 130.2 | 130.2 | 1449 |
| M7 | Baja, E coast | Gulf of California | 17.5 | 1.7 | 9.6 | 993 |
| M8 | Mexico, W coast | Gulf of California | 17.5 | 1.7 | 9.6 | 1097 |
| M9 | Greenland, E coast, NE corner | Arctic | 59.8 | 13.5 | 36.65 | 758 |
| M10 | Greenland, E coast (north) | North Atlantic | 56.8 | 55.9 | 56.4 | 737 |
| M11 | Greenland, E coast (central) | North Atlantic | 38.6 | 30.6 | 34.6 | 565 |
| M12 | Greenland, E coast (south) | North Atlantic | 63.8 | 58.8 | 61.3 | 1244 |
| M13 | Greenland, W coast | Labrador Sea | 89.5 | 87.5 | 88.5 | 1126 |
| M14 | North America, Labrador coast | Labrador Sea | 109 | 68 | 88.5 | 1540 |
| M15 | N America, E coast (Grand Banks) | Central Atlantic | 129 | 127 | 128.0 | 951 |
| M16 | N America, E coast (S side Grand Banks) | Central Atlantic | 150.9 | 134.7 | 149.5 | 493 |
| M17 | N America, E coast (United States) | Central Atlantic | 171 | 170 | 170.5 | 2889 |
| M18 | Bahama plateau, N margin | Central Atlantic | 170 | 146 | 158.0 | 637 |
| M19 | S America, N coast (Guyana) | South Atlantic | 103.8 | 94 | 98.9 | 813 |
| M20 | S America, N coast (Amazon) | South Atlantic | 109.7 | 102.1 | 105.9 | 2434 |
| M21 | S America, E coast (Argentina) | South Atlantic | 134.8 | 109.6 | 122.2 | 5198 |
| M22 | Falkland plateau, N margin | South Atlantic | 134.3 | 116.7 | 125.5 | 1295 |
| M23 | Falkland plateau, SE margin | South Atlantic | 139.8 | 138.9 | 139.4 | 725 |
| M24 | Jan Mayen plateau, N margin | North Atlantic | 57.3 | 34.7 | 46.0 | 156 |
| M25 | Jan Mayen plateau, E margin | North Atlantic | 59.3 | 52.4 | 55.9 | 641 |
| M26 | Jan Mayen plateau, S margin | North Atlantic | 52.4 | 35.4 | 43.9 | 133 |
| M27 | Jan Mayen plateau, W margin | North Atlantic | 35.4 | 35.4 | 35.4 | 582 |
| M28 | Svalbard, S margin | North Atlantic | 46.6 | 14.6 | 30.6 | 790 |
| M29 | Europe, W coast (Norwegian Sea) | North Atlantic | 58.6 | 46.7 | 52.7 | 976 |
| M30 | Europe, margin W of Shetlands facing Jan Mayen | North Atlantic | 59.3 | 52.4 | 55.9 | 528 |
| M31 | Europe, margin W of Ireland facing Iceland | North Atlantic | 59.9 | 56.5 | 58.2 | 1336 |
| M32 | Europe, margin SW of Ireland | Central Atlantic | 108.7 | 82.6 | 95.6 | 1236 |
| M33 | Europe, W coast, France | Bay of Biscay | 108.7 | 102.2 | 105.4 | 806 |
| M34 | Iberia, W coast | Central Atlantic | 129.7 | 119.5 | 124.6 | 792 |
| M35 | Africa, W coast (Mauritania) | Central Atlantic | 171.4 | 167.2 | 169.3 | 3169 |
| M36 | Africa, W coast (Guinea) | Central Atlantic | 109.9 | 109.5 | 109.7 | 2545 |
| M37 | Africa, W coast (Namibia) | South Atlantic | 133.6 | 119.9 | 126.8 | 5067 |
| M38 | Africa, S coast (Agulhas) | Southern | 143.6 | 126.6 | 135.1 | 1316 |
| M39 | Africa, E coast (Mozambique) | Indian | 179.6 | 179.3 | 179.5 | 1472 |
| M40 | Africa, E coast (Mozambique E of M39) | Indian | 174.5 | 158.5 | 166.5 | 546 |
| M41 | Madagascar, W coast | Mozambique Channel | 169.9 | 169.5 | 169.7 | 1431 |
| M42 | Madagascar, SW end | Mozambique Channel | | | 132.9 | 490 |
| M43 | Madagascar, E coast | Indian | 103.5 | 99.1 | 101.3 | 1448 |
| M44 | Madagascar, NE corner | Indian | | | 134.3 | 228 |
| M45 | Africa, E coast (Dar Es Salaam) | Indian | 169.7 | 156.3 | 163.0 | 966 |
| M46 | Africa, E coast (Somalia) | Indian | 169.8 | 168.9 | 169.3 | 1992 |
| M47 | Africa, N coast (Somalia) | Gulf of Aden | 29.8 | 28.5 | 29.2 | 1289 |
| M48 | Egypt, E coast | Red Sea | 5 | 5 | 5.0 | 1591 |
| M49 | Arabia, W coast | Red Sea | 5 | 5 | 5.0 | 1615 |
| M50 | Arabia, S coast (Yemen) | Gulf of Aden | 29.4 | 28.5 | 29.0 | 1716 |
| M51 | Arabia, E end (33–75 Ma) | Arabian Sea | 33 | 75 | 54.0 | 585 |
| M52 | India, W coast | Arabian Sea | 119.4 | 98.6 | 109.0 | 2295 |
| M53 | India, SE tip facing Sri Lanka | Indian, Gulf of Mannar | 128.1 | 122.2 | 125.2 | 298 |
| M54 | Sri Lanka, W coast facing SE tip of India | Indian, Gulf of Mannar | 128.1 | 120.8 | 124.5 | 331 |
| M55 | Sri Lanka, S coast | Indian | 120.2 | 119.6 | 119.9 | 323 |
| M56 | Sri Lanka, NE coast | Indian, Bay of Bengal | 127.8 | 119.8 | 123.8 | 341 |
| M57 | India, E coast N of Sri Lanka | Indian, Bay of Bengal | 128.1 | 120.4 | 124.3 | 1812 |
| M58 | N Korea, E margin | Japan Sea | 28 | 28 | 28 | 620 |
| M59 | China, SE margin, Hainan to Taiwan | South China Sea | 31 | 31 | 31 | 390 |
| M60 | Macclesfield Bank E of Vietnam, SE side | South China Sea | 27 | 19 | 23 | 550 |
| M61 | Australia, NW coast (Broome) | Indian | 150.6 | 140.1 | 145.4 | 844 |
| M62 | Australia, NW coast (N margin Exmouth Plat.) | Indian | 150.9 | 134.7 | 142.8 | 403 |
| M63 | Australia, W coast N of Perth | Indian | 134.2 | 128.3 | 131.3 | 1897 |
| M64 | Naturaliste Plateau, W of Perth, N margin | Indian | 126 | 132 | 129.0 | 397 |
| M65 | Naturaliste Plateau, W of Perth, W margin | Indian | 130 | 130 | 130.0 | 199 |
| M66 | Australia, S coast, western part | Southern | 89.2 | 82.7 | 86.0 | 2576 |
| M67 | Tasmania, W coast | Southern | 64.9 | 33.8 | 49.4 | 1658 |
| M68 | Australia, E coast | Coral–Tasman | 89.3 | 72.9 | 81.1 | 4128 |
| M69 | Lord Howe Rise, W margin | Coral–Tasman | 84.5 | 72.9 | 78.7 | 5123 |
| M70 | Campbell Plateau, S margin (R edge of map) | Southern | 87.4 | 87 | 87.2 | 1183 |
| M70 | Campbell Plateau, S margin (L edge of map) | Southern | 87.4 | 87 | 87.2 | 139 |
| M71 | Chatham Rise, S margin (R edge map) | Southern | 80 | 80 | 80.0 | 377 |

Author's personal copy



**Table 1** (*continued*)

| Number | Margin name | Ocean | Oldest age (Ma) | Youngest age (Ma) | Mean age (Ma) | Length (km) |
|---|---|---|---|---|---|---|
| M71 | Chatham Rise, S margin (L edge map) | Southern | 80 | 80 | 80.0 | 755 |
| M72 | Antarctica facing Pacific | Southern | 87.4 | 80 | 85.0 | 2898 |
| M73 | Antarctica, S of Africa | Southern | 179.6 | 120.4 | 134.6 | 5381 |
| M74 | Antarctica, S of Australia | Southern | 89.2 | 82.7 | 86.0 | 2591 |
| M75 | Antarctica, S of Tasmania | Southern | 64.9 | 33.8 | 49.4 | 1564 |

ratings of "B", the quoted lifespans have been rounded to the nearest 5 m.y., for margins with a rating of "C", lifespans are rounded to the nearest 10 m.y. A rating of "D" is given to supposed passive margins for which a lifespan cannot even be estimated. Some margins in this category are quite controversial but are included nonetheless, with caveats. In general, local experts would likely bestow higher quality ratings than I have—a lifetime of study of a given margin will obviously lead to a deeper appreciation of the age constraints than I have been able to glean during this broad sysnthesis. The write-up for each margin explains my reasons for choosing the start dates and end dates.

Not all of the eighty-five margins of the complete dataset are amenable to the same treatment. For most of the margins, a numerical age can be set for both the start date and end date, and these are assigned to Group 1 in Table 2 ($n=76$). Group 2 includes a few margins for which the end date is known, but not the start date ($n=5$). Group 3 the remaining margins for which neither a start date nor end date is known ($n=4$).

## 3. Modern passive margins

The locations and ages of the present-day passive margins are evident from world maps of bathymetry, seismicity, and magnetic anomalies. Fig. 3 shows the distribution of modern margins and Table 1 summarizes their lengths and ages. The cited age of each margin is the age of the oldest flanking magnetic anomaly. Margins that formed diachronously by rift propagation were subdivided into age sectors and a mean age is cited for each sector. Lengths of modern margins were taken as the great-circle distance between endpoints.

The present Earth has about 105,000 km of passive margins (Fig. 3). They range in age from ca. 5 m.y. (Red Sea) to ca. 180 m.y. (Mozambique sector of Africa's east coast) (Fig. 4 and Table 1). The mean age of all the modern passive margins, weighted by length, is about 104 m.y.

## 4. Ancient passive margins

Table 2 lists the start date, end date, lifespan, and quality ranking of the ancient passive margins. These data are plotted in Fig. 5 and the margins are located in Fig. 6. Four margins are discussed at length in the main body of the paper: a modern-day collision (northern Australia), a classic Phanerozoic example (the Cambrian–Ordovician Appalachian margin of Laurentia), the longest-lived example (Mesoproterozoic eastern margin of the Siberian craton), and the oldest example that has sound age constraints (Kaapvaal craton). The rest are described in variable detail in the Appendix.

### *4.1. Present-day collision between Australia and the Banda forearc*

Northern Australia was entirely rimmed by passive margins from the Cretaceous to the Oligocene when the eastern sector collided with an arc in New Guinea (Appendix, margin A80). The western part of the northern margin (margin A79) survived as a passive margin until a few million years ago when it began colliding with the Banda forearc (Fig. 7) (*e.g.*, Karig et al., 1987). The trend of the yet-to-collide part of the passive margin is oblique to that of the trench, and the collision tip is thus propagating westward. Pre-collisional conditions along the passive margin, forearc, and arc can be seen west of the collision tip (Fig. 7).

Australia's northern and western margins experienced a protracted history involving departure of a series of blocks during the

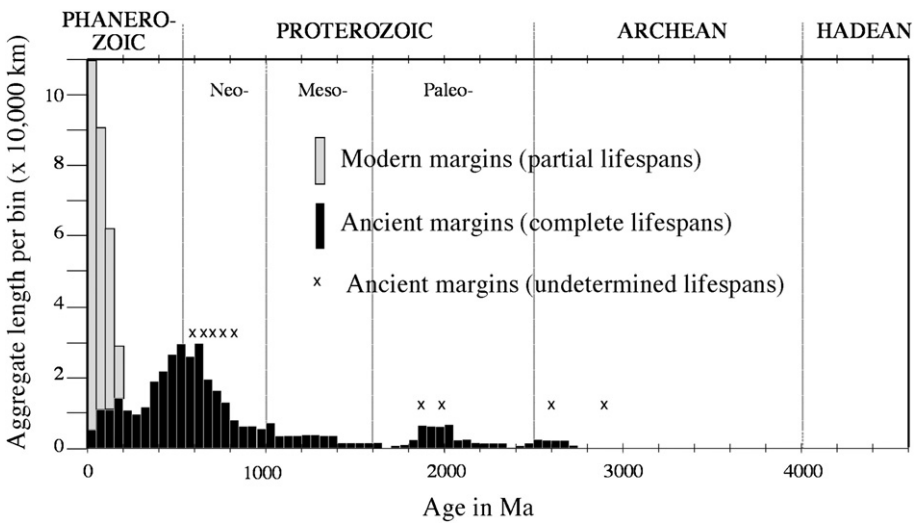


**Fig. 4.** Histograms showing the age distribution of ancient and modern passive margins using data in Tables 1 and 2. Bins are 50 m.y. in duration and each margin is weighted by length. Thus, a particular 1000-km-long passive margin that existed from 525 to 375 Ma would contribute 1000 km to the height of four consecutive bins.

Author's personal copy



**Table 2**
Summary data for ancient passive margins as described in text and Appendix. "Group" refers to the subset of data used for plots and calculations as discussed in Section 2.5. Asterisk indicates a rounded value. Locations are given in Fig. 6

| Number | Group | Margin and orogen | Where | Start date (Ma) | End date (Ma) | Lifespan (m.y.) | Quality | High-P metamorphism? | Foredeep magmatism? | Length (km) |
|---|---|---|---|---|---|---|---|---|---|---|
| A1 | 1 | Arctic Alaska microcontinent, S side, Brookian orogen | Alaska, Russia | 350 | 170 | 180 | A | Y | N | 1230 |
| A2 | 1 | Farewell terrane | Alaska | 545 | 435 | 110 | C | N | N | 460 |
| A3 | 1 | Laurentian craton, W side, northern sector, Antler orogen | Canada | 710 | 385 | 325 | B | N | Y | 1560 |
| A4 | 1 | Laurentian craton, W side, southern sector, Antler orogen | USA, Canada | 542 | 357 | 185 | A | N | Y | 1870 |
| A5 | 1 | Laurentian craton, N side, Innuitian margin, Ellesmerian orogen | Canada, Greenland | 620 | 444 | 180* | C | N | N | 1900 |
| A6 | 1 | Slave craton, W side, Wopmay orogen | Canada | 2015 | 1883 | 132 | A | N | Y | 560 |
| A7 | 1 | Slave craton, E side, Kimerot platform, Thelon orogen | Canada | 2090 | 1970 | 120 | C | N | N | 630 |
| A8 | 1 | Laurentian craton, N side, Borden Basin, Poseidon orogen | Canada | 1255 | 1200 | 55 | C | N | N | 270 |
| A9 | 1 | Hearn craton, SE side | Canada | 2070 | 1880 | 190 | B | N | Y | 820 |
| A10 | 3 | Steep Rock Lake platform, Superior Craton, Wabigoon Province | Canada | Unk (<3002) | Unk (<2870) | Unk | D | N | N | 15 |
| A11 | 1 | Wyoming Craton, S side, Medicine Bow orogen | USA | 2000 | 1780 | 220 | B | N | N | 310 |
| A12 | 1 | Superior craton, S side, Huronian margin, Penokean orogen | Canada, USA | 2300 | 2065 | 235 | C | N | NA | 1170 |
| A13 | 1 | Superior craton, S side, Animike margin, Penokean orogen | Canada, USA | 2065 | 1880 | 185 | B | N | Y | 1170 |
| A14 | 1 | Superior Craton, N side, Cape Smith and Trans-Hudson orogens | Canada | 2000 | 1875 | 125 | B | N | Y | 370 |
| A15 | 1 | Superior craton, E side, New Quebec orogen e ("Labrador Trough") | Canada | 2135 | 1890 | 245 | B | N | Y | 960 |
| A16 | 2 | Nain craton, W margin, Torngat orogen | Canada | Unk (>1876) | 1859 | Unk | D | N | N | 290 |
| A17 | 1 | Nain Craton, N side, Makkovik orogen | Canada | 2175 | 2010 | 165 | C | N | N | 110 |
| A18 | 1 | Laurentian craton, S side, Ouachita orogen | USA | 520 | 310 | 210 | A | N | N | 1720 |
| A19 (a, b) | 1 | Laurentian craton, E side, Appalachian margin, Taconic orogen (a) and NW Scotland (b) | USA, Canada | 540 | 465 | 75 | A | Y | Y | 3320 |
| A20 (a,b) | 1 | Laurentian craton, E side, E Greenland (a) and NE Svalbard (a) | Greenland, Svalbard | 815 | 444 | 370* | C | Y | N | 1740 |
| A21 | 1 | Baltic Craton, W side, Scandinavian Caledonide orogen | Norway | 605 | 505 | 100 | A | Y | N | 1550 |
| A22 | 1 | Kola craton, S side, Kola suture belt | Russia | 1970 | 1800 | 170 | B | N | N | 690 |
| A23 | 1 | Baltic craton, N side, Timanides | Russia | 1000 | 560 | 440 | C | N | N | 1460 |
| A24 | 1 | Baltic craton, E side, Uralian orogen, Phase 1 | Russia | 1000 | 620 | 380 | B | Y | N | 1000 |
| A25 | 1 | Baltic Craton, E side, Uralian orogen, Phase 2 | Russia | 477 | 376 | 101 | A | N | N | 3130 |
| A26 | 1 | Baltic craton, S side, Variscan orogen | Ireland to Poland | 407 | 347 | 60 | A | Y | Y | 1080 |
| A27 | 1 | Saxo-Thuringian block | Germany | 444 | 344 | 100 | B | N | N | 400 |
| A28 | 1 | S margin of Europe, Alpine orogen | Switzerland | 170 | 43 | 127 | A | Y | N | 790 |
| A29 | 1 | Pyreneean-Biscay margin of Iberia | Spain | 115 | 70 | 45 | A | N | N | 390 |
| A30 | 1 | NW Iberia, Variscan orogen | Spain | 475 | 385 | 90 | B | N | Y | 210 |
| A31 | 1 | Apulian microcontinent, Pindos ocean | Greece | 230 | 60 | 170 | A | Y | N | 630 |
| A32 | 1 | Isparta angle, western margin | Turkey | 227 | 60 | 167 | A | Y | N | 280 |
| A33 | 1 | Isparta angle, eastern margin | Turkey | 227 | 53 | 174 | A | Y | N | 260 |
| A34 | 1 | Arabia, NE margin, Oman-Zagros orogen | Oman, Iran | 272 | 87 | 185 | A | Y | N | 2300 |
| A35 | 1 | Alborz orogen | Iran | 390 | 210 | 170 | B | N | N | 550 |
| A36 | 2 | Siberian craton, N side, Taymyr, Phase 1 | Russia | >750 | 600 | >150 | D | N | N | 1380 |
| A37 | 1 | Siberian craton, N side, Taymyr, Phase 2 | Russia | 530 | 325 | 205 | B | N | N | 1380 |
| A38 | 1 | Siberian craton, W side, Yenisei Ridge | Russia | 1350 | 850 | 500 | C | N | N | 1910 |
| A39 | 3 | Gargan microcontinent, W side | Russia, Mongolia | Neoprot. | Neoprot | Unk | D | N | N | 150 |
| A40 | 1 | Siberian craton, S side, Baikal | Russia | 1000 | 600 | 400 | C | N | N | 1160 |
| A41 | 1 | Dzabkhan block | Mongolia | 710 | 580 | 130 | B | N | N | 200 |
| A42 | 3 | Idermeg terrane | Mongolia | Neoprot. | Mid-Camb. | Unk | D | N | N | 300 |
| A43 | 1 | Karakorum block | Pakistan | 268 | 193 | 75 | B | N | N | 500 |
| A44 | 1 | Tarim microcontinent, N side, Tien Shan orogen | China | 600 | 380 | 220 | C | N | N | 1320 |
| A45 | 1 | Tarim microcontinent, S side, Kunlun orogen | China | 600 | 430 | 170 | B | N | N | 950 |
| A46 | 1 | Indian craton, N side, Himalayan orogen, Phase 1 | India, Nepal | 635 | 502 | 133 | A | N | N | 2460 |
| A47 | 1 | Indian craton, N side, Himalayan orogen, Phase 2 | India, Nepal | 271 | 52 | 219 | A | Y | N | 2460 |
| A48 | 1 | Aravelli-Delhi orogen | India | 2000 | 1800 | 200 | C | N | N | 740 |
| A49 | 1 | South China Craton, NW side, Longmen Shan orogen, Phase 1 (ended by re-rifting) | China | 600 | 300 | 300 | C | N | NA | 480 |
| A50 | 1 | South China Craton, NW side, Longmen Shan orogen, Phase 2 | China | 300 | 228 | 72 | B | N | N | 480 |
| A51 | 1 | North China craton, Central orogenic belt | China | 2740 | 2530 | 210 | C | N | N | 900 |
| A52 | 1 | South China Craton, N side, Qinling–Dabie orogen, Phase 1 | China | 750 | 440 | 310 | C | N | N | 560 |
| A53 | 1 | South China Craton, N side, Qinling–Dabie orogen (2) | China | 360 | 235 | 125 | C | Y | N | 560 |
| A54 | 1 | South China craton, SE side, Nanling orogen | China | 635 | 445 | 190 | B | N | N | 1730 |
| A55 | 1 | China, E side, Taiwan orogen | Taiwan | 28 | 5 | 23 | A | Y | Y | 500 |

Author's personal copy



**Table 2** (*continued*)

| Number | Group | Margin and orogen | Where | Start date (Ma) | End date (Ma) | Lifespan (m.y.) | Quality | High-P metamorphism? | Foredeep magmatism? | Length (km) |
|---|---|---|---|---|---|---|---|---|---|---|
| A56 | 1 | Siberian craton, E side, Verkhoyansk orogen, Phase 1 | Russia | 1600 | 1010 | 590 | C | N | Y | 1700 |
| A57 | 1 | Siberia, E side, Verkhoyansk, Phase 2 (ended by re-rifting) | Russia | 650 | 380 | 270 | C | N | NA | 1700 |
| A58 | 1 | Siberia, E side, Verkhoyansk, Phase 3 | Russia | 380 | 160 | 220 | C | N | N | 1700 |
| A59 | 1 | Guaniguanico terrane | Cuba | 159 | 80 | 79 | A | N | N | 150 |
| A60 | 1 | S. American Craton, N side, Venezuela margin | Venezuela | 159 | 34 | 125 | A | Y | N | 1080 |
| A61 | 1 | Amazon craton, SE side, Araras margin, Paraguay orogen | Brazil | 640 | 580 | 60 | B | N | N | 470 |
| A62 | 1 | Cuyania terrane, Argentine Precordillera, E side | Argentina | 530 | 473 | 57 | A | N | N | 640 |
| A63 | 1 | Sao Francisco craton, W side, Brasiliano orogen | Brazil | 745 | 640 | 105 | B | N | N | 1080 |
| A64 | 1 | Sao Francisco craton, E side, Aracauai–Ribeira orogen | Brazil | 900 | 590 | 310 | B | N | N | 750 |
| A65 | 1 | Sao Francisco craton, S side, Transamazonian orogen | Brazil | 2500 | 2130 | 370 | C | N | N | 200 |
| A66 (a,b,c) | 1 | Sierra de la Ventana (a), Cape (b), and Ellsworth Mtns. (c) | Argentina, S. Africa, Antacrtica | 500 | 300 | 200 | B | N | N | 2170 |
| A67 | 1 | West African craton, N side, Anti-Atlas orogen | Morocco | 800 | 580 | 220 | C | N | N | 560 |
| A68 | 1 | West African craton, W side, Mauritanide orogen | Mauritania | 675 | 650 | 25 | C | N | N | 1692 |
| A69 | 1 | West African craton, E side, Dahomeyide orogen | Ghana, Mali | 775 | 625 | 150 | C | Y | N | 2200 |
| A70 | 2 | LATEA craton, Hoggar, W side | Algeria, Mali | Unk | 870 | Unk | D | NA | NA | 840 |
| A71 | 2 | LATEA craton, Hoggar, S side | Algeria, Niger | Unk | 685 | Unk | D | NA | NA | 550 |
| A72 | 1 | East Africa Orogen, W side | Sudan | 840 | 730 | 110 | C | N | N | 1460 |
| A73 | 1 | Congo Craton, W side, Kaoko Belt (N Coastal Branch) of Damara orogen | Namibia | 780 | 580 | 200 | A | N | N | 2175 |
| A74 | 1 | Congo Craton, S side, Inland Branch, Damara orogen | Namibia | 670 | 555 | 115 | A | N | N | 1800 |
| A75 | 1 | Kalahari Craton, N side, Inland Branch, Damara orogen | Namibia | 670 | 550 | 120 | A | N | N | 540 |
| A76 | 1 | Kalahari Craton, W side, Gariep Belt, (S Coastal Branch) of Damara orogen | Namibia | 735 | 535 | 200 | A | N | N | 690 |
| A77 | 1 | Kaapvaal Craton, W side | S. Africa, Botswana | 2640 | 2470 | 170 | C | N | N | 810 |
| A78 | 3 | Zimbabwe craton, S side, Belingwe greenstone belt | Zimbabwe | ca. 2600 | ca. 2600 | Unk | D | N | N | 60 |
| A79 | 1 | Australian craton, NW side, Timor orogen | Indonesia | 151 | 4 | 147 | A | Y | N | 1530 |
| A80 | 1 | Australian craton, NE side, New Guinea orogen | New Guinea, Irian Jaya | 180 | 26 | 154 | A | N | Y | 1380 |
| A81 | 1 | Northwest Australia craton, Halls Creek orogen | Australia | 1880 | 1860 | 20 | C | N | N | 270 |
| A82 | 2 | Rudall Complex | Australia | >2000 | 1780 | >220 | D | N | N | 330 |
| A83 | 1 | Pilbara Craton, S margin, Ophthalmian orogen | Australia | 2685 | 2445 | 240 | B | N | Y | 580 |
| A84 | 1 | Gawler Craton, NE side, Kimban orogen | Australia | 1900 | 1740 | 160 | C | N | N | 650 |
| A85 | 1 | Australia, E side, Tasman orogen | Australia | 590 | 520 | 70 | B | N | N | 1670 |

Paleozoic and Mesozoic (Longley et al., 2002). Just southwest of the collision tip (Fig. 7), the age of the rift-drift transition is evident from the oldest seafloor adjacent to the continent (ca. 155 Ma; Longley et al., 2002). Longley et al. (2002, their Figs. 10 and 15) interpreted this sector of the passive margin to be related to the rifting away of the Argo microplate. East of the collision tip (Fig. 7), the already collided portion of the passive margin is interpreted to have a slightly younger rift-drift transition, related to separation of a part of the West Burma block at about the Kimmeridgian–Tithonian boundary (ca. 151 Ma) in the Late Jurassic (Longley et al., 2002, their Figs. 7 and 10). At the collision tip, the distance from Australia's shoreline to the ocean–continent boundary is about 500 km (Longley et al., 2002); this gives an indication of the distances that might be involved in reconstructing stratigraphy across an ancient passive margin and foredeep.

The present-day Java Trench can be tracked directly into Timor Trough, establishing the continuity between the pre-collisional subduction trench and the syncollisional foredeep. The former, floored by Jurassic seafloor, is 6–7 km deep, whereas the latter, floored by Australian continental crust, is only 2–3 km deep. At DSDP Site 262 in the axis of Timor Trough, modern trench sediments depositionally overlie Pliocene shallow-marine carbonates (Veevers et al., 1978), demonstrating that the Australian margin has subsided in only a few million years to abyssal depths. The southern margin of Timor Trough is cut by young normal faults. These have been interpreted as the product of collision-induced flexure of the downgoing plate and not the product of classic rifting related to plate divergence (Bradley and Kidd, 1991). A discontinuous forebulge is evident on the downgoing passive-margin plate, most notably at Kepulauan Aru where Neogene shelf deposits have been broadly upwarped along an arch that parallels the trench (Bradley and Leach 2003) (Fig. 7).

The northern wall of Timor Trough is an actively deforming submarine orogen (Karig et al., 1987). Although much of the collisional orogen lies below sea level, it is emergent on the island of Timor, where an ocean-floor sedimentary sequence that ranges from Neocomian to Miocene was thrust onto the Australian margin in mid-Pliocene time (ca. 4 Ma) (Carter et al., 1976, p. 184). An important feature of the present-day collision is that the magmatic axis of the Banda Arc is far from the collision zone, separated from the orogen in Timor by a deep forearc basin, the Savu Basin. Substantial orogenic shortening will need to happen if the magmatic arc itself is ever to come close to the passive margin.

Age controls for this relatively young margin are tighter than they are for most of the other ancient margins. The rift-drift transition was at ca. 151 Ma and the onset of collision was at about 4 Ma, yielding a lifespan of about 147 m.y. This is probably accurate to within about 10 m.y. and applies to a 1500-km-long section of passive margin.

Author's personal copy



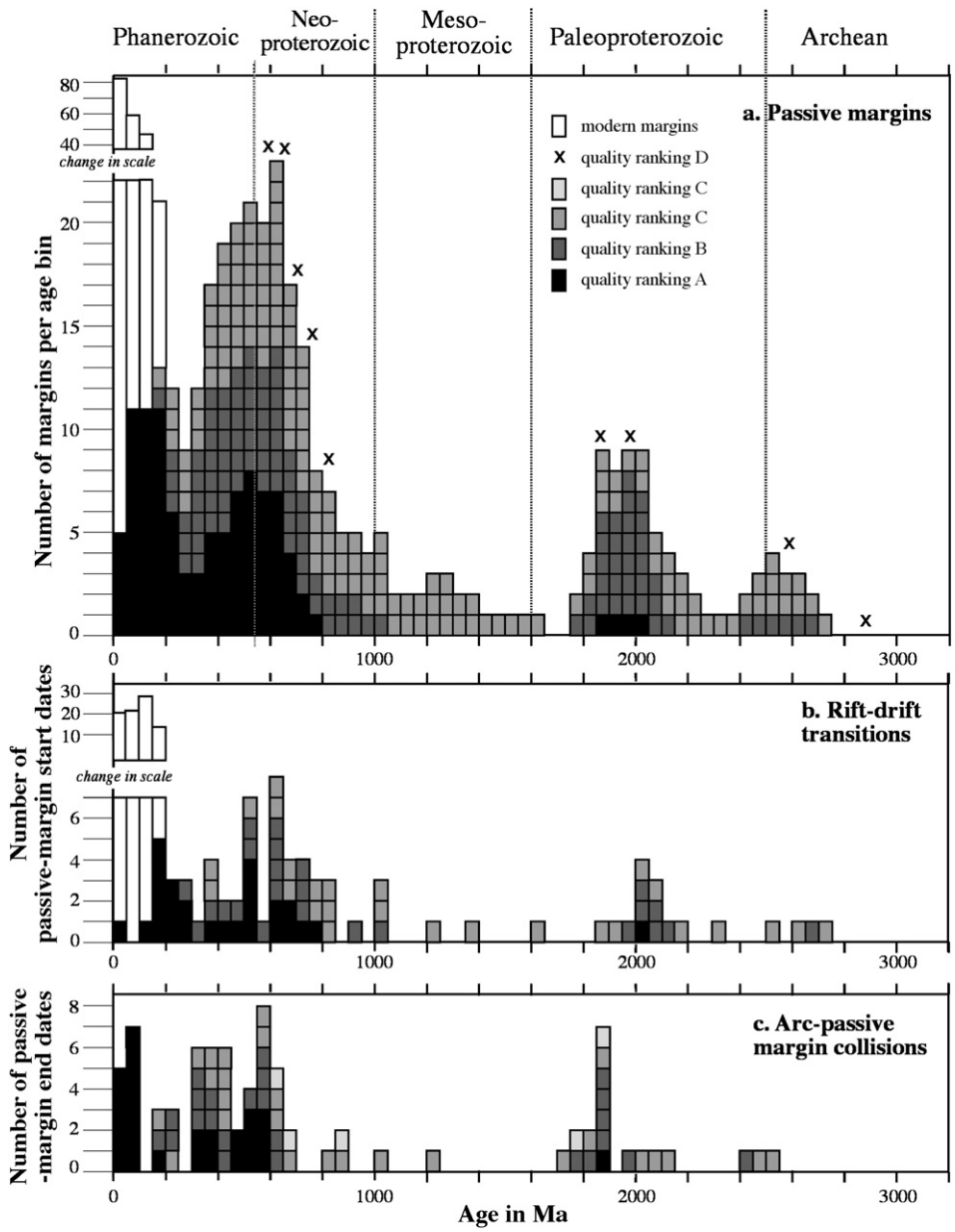


**Fig. 5.** Histograms showing age distributions of the ancient margins, from data in Table 2. Quality rankings are color coded. (a) Number of margins per 50-m.y. time bin. Each margin appears in anywhere from one to twelve consecutive histogram bins, depending on its lifespan. For example, a margin with a start date of 550 Ma and an end date of 475 Ma will show up in the 550–600, 500–550, and 450–500 Ma bins. Based on Group 1 data; $n=76$. Also plotted (x symbol) are the 9 margins having quality rankings of D. Except for the oldest one (Steep Rock Lake, margin A10), these amplify rather than modify the age distribution shown by the better-dated margins. (b) Times of rift-drift transition, based on Group 1 data (76 ancient margins) and 75 modern margins. (c) Times of arc–passive margin collision, based on Group 1 and Group 2 data; $n=81$.

### *4.2. Cambrian–Ordovician Appalachian margin of Laurentia*

The Appalachian margin of eastern Laurentia (margin A19a) is one of the most thoroughly studied and well understood Phanerozoic passive margins. No margins in the unfossiliferous Proterozoic boast such extraordinary age control. The Appalachian margin extends a distance of about 3300 km from easternmost Canada to the southeastern United States. In the southeastern United States, Laurentia's Appalachian margin swings west and becomes the Ouachita segment; this segment has a different history from the Appalachians and is discussed separately (margin A18). On a fit of the Atlantic continents, a continuation of the Appalachian margin is recognized in northwestern Scotland (margin A19b); this segment is not discussed further but has a history similar to that of Newfoundland (van Staal et al., 1998; Cawood et al., 2007A). The portion of the margin within the United States was summarized in comprehensive reviews by Rankin et al. (1989), Read (1989), and Drake et al. (1989). The Canadian portion was likewise covered by Williams et al. (1995), Knight et al. (1995), Hiscott (1995), and Williams (1995). The following discussion focuses on two transects: (1) Newfoundland (Fig. 8b), where all the main phases of passive-margin evolution–rifting, thermal subsidence, and collision–are clearly legible in the rock record, and (2) northern New York (Fig. 8c), where the foredeep is especially well exposed on the flanks of a Neogene dome, the Adirondack Mountains.

Granulite-facies metamorphic rocks and plutonic rocks form the basement to the passive margin. These rocks belong to the 1.3 to 1.0-Ga Grenville Province (Rivers, 1997) and occur both as autochthonous

Author's personal copy



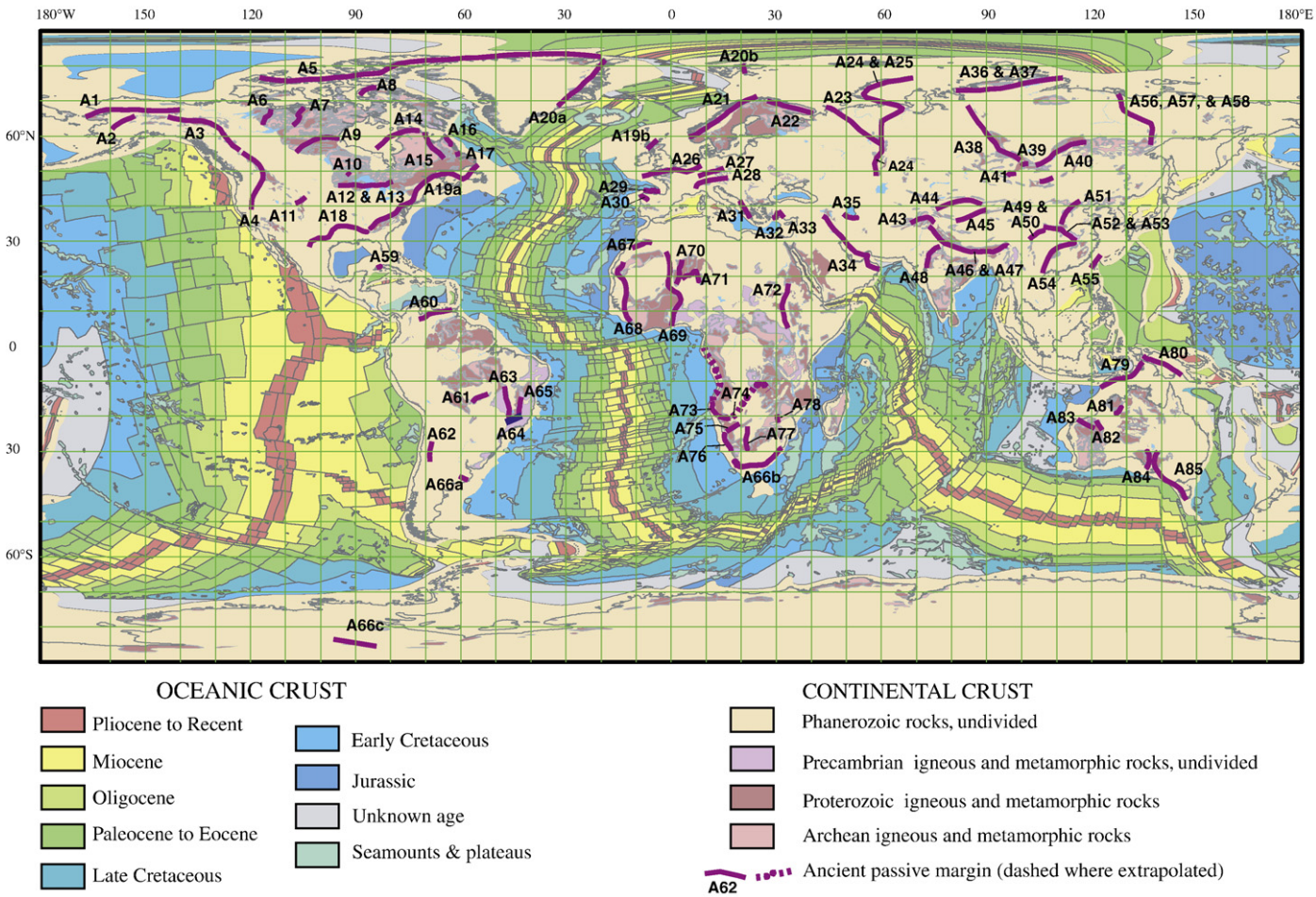


**Fig. 6.** World map showing ancient passive margins. The ancient margins are labeled A1 to A85 from northwest to southeast. A few superimposed passive margins are shown as a single line but have more than one number. Base map from Commission de la Carte Géologique du Monde (2000).

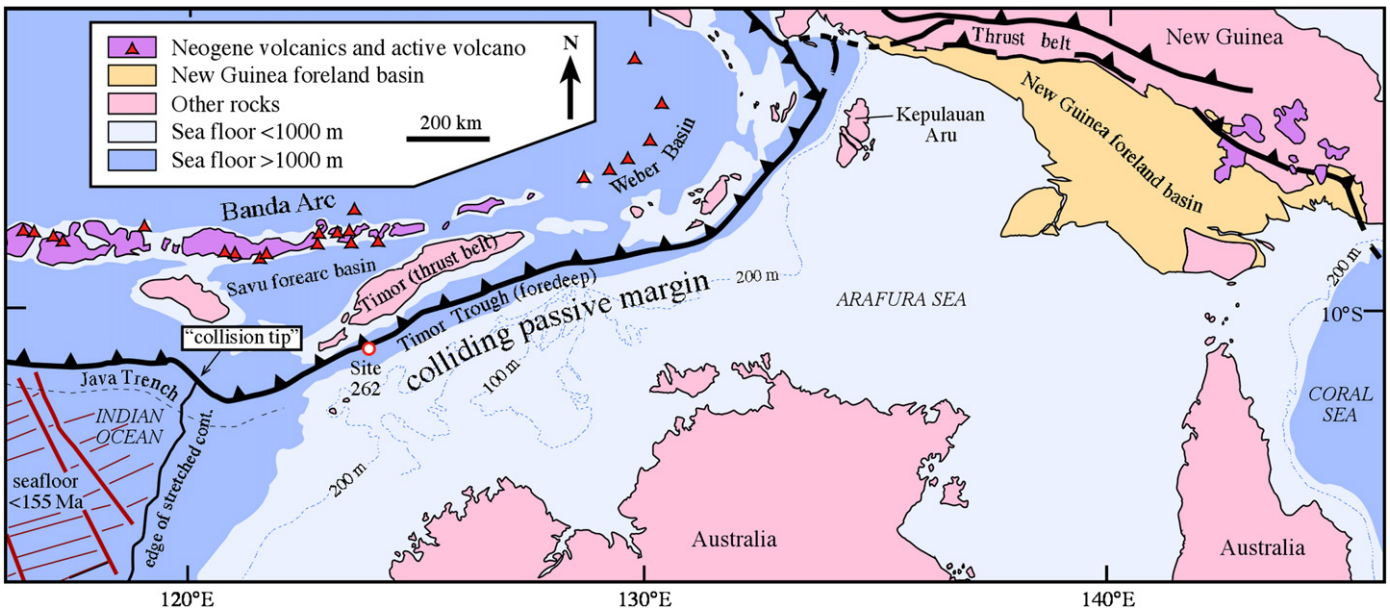


**Fig. 7.** Generalized tectonic map of the ongoing collision zone between Australia's northwestern passive margin and the Banda Arc. West of the point labeled "collision tip", oceanic crust of the Australian plate is subducting beneath the Banda Arc at the Java Trench, and the Australian passive margin is obliquely approaching the subduction zone. Immediately east of the collision tip, collision has just begun and involves stretched continental crust. Farther east, collision has been underway since 4 Ma and a collisional orogen has grown to heights approaching 3 km. Timor Trough is an underfilled syncollisional foredeep that can be traced into the Java Trench. Adapted from Hamilton (1979).

Author's personal copy



basement and in thrust sheets (Fig. 8a). Upper Neoproterozoic rift-related sedimentary and igneous rocks are recognized at many places along the length of the margin, and are attributed to rifting on the basis of sedimentary facies, age, igneous components, and chemistry (Rankin et al., 1989; Williams et al., 1995). In Newfoundland (Fig. 8b), Grenville basement is unconformably overlain by upper Neoproterozoic arkoses, conglomerates, quartzites, graywackes, and columnar and pillowed lavas (Williams et al., 1995). Abrupt changes in thickness and stratigraphic order are consistent with local, fault control of deposition. Tholeiitic mafic dikes are related to the flows and attest to significant extension; the dikes strike northeast, parallel to the eventual passive margin (Williams et al., 1995). Rift-related igneous rocks are as old as 617±8 Ma (Hare Hill alkaline granite; Williams et al., 1995), and as young as 550.5+3/−2 Ma (lavas of the Skinner Cove Formation; Cawood et al., 2001). The youngest detrital zircons in rift-related strata, at 572 Ma (Cawood and Nemchin, 2001), are not much older than the youngest lavas.

The succeeding Cambrian to Ordovician platformal sequence is one of the world's classic miogeoclinal prisms. The platformal strata thicken to the east, deepen to the east, and blanket slightly older rift-related rocks—all pointing toward a passive-margin setting. In Newfoundland, the lower part of the sequence consists of sandstone, siltstone, shale, and limestone, and the upper part is limestone and dolomite. Being gradual, the transition from extension-driven to thermally driven subsidence is impossible to pinpoint, but clearly it had taken place by late Early Cambrian (ca. 520 Ma; Knight et al., 1995,

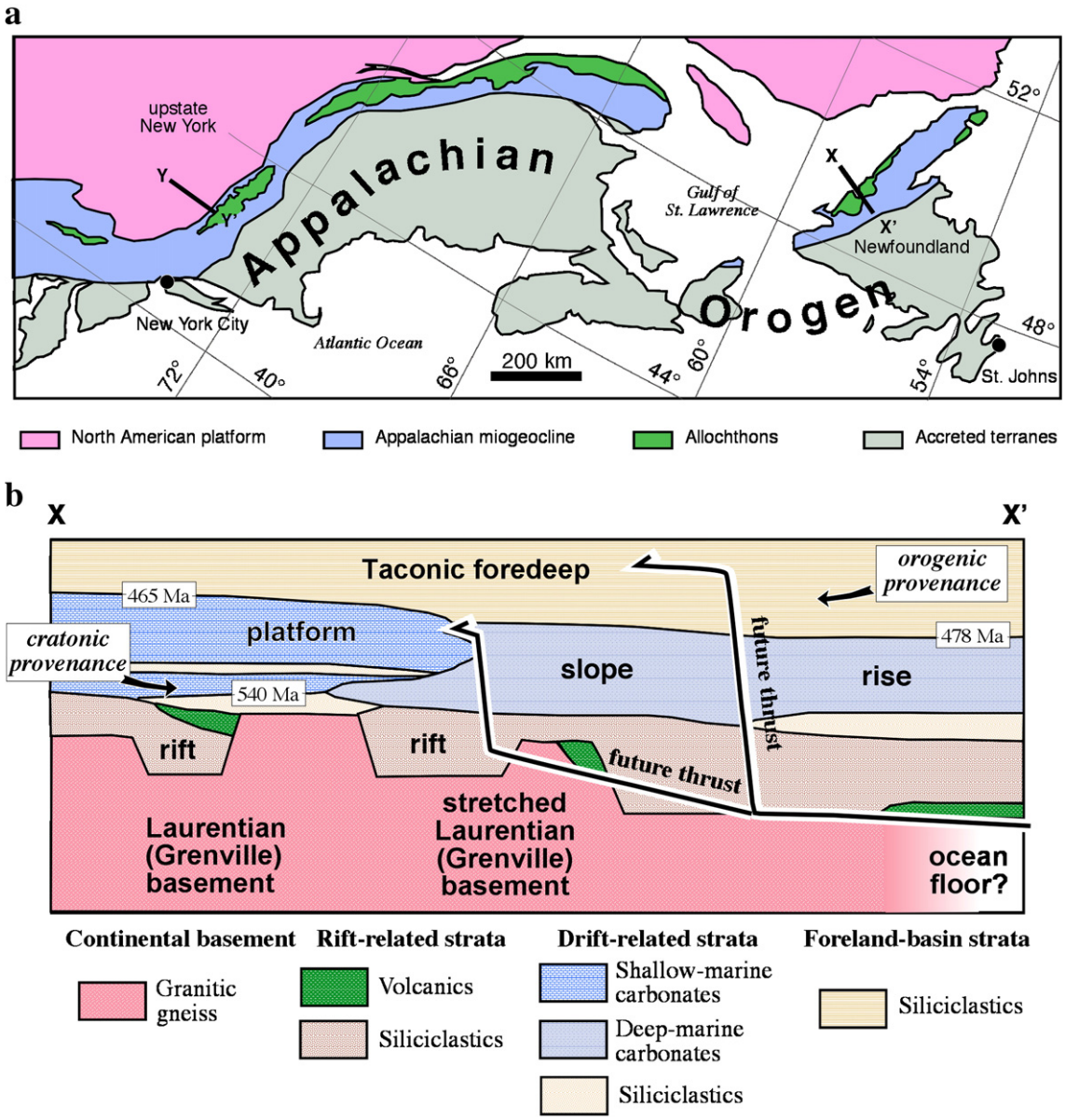


**Fig. 8.** (a) Map of the Northern Appalachian orogen showing the lines of two cross-sections, from Cawood and Nemchin (2001). (b) Stratigraphic cross-section across the Cambrian–Ordovician passive margin in Newfoundland, adapted from Cawood and Nemchin (2001). Note the sequence of rift-passive margin, and foreland basin, and the west-to-east deepening in the passive-margin succession. (c) Stratigraphic cross-section of the foreland basin in northern New York emphasizing age relations, adapted from Bradley (1989) and Landing and Bartowski (1996). The foreland-basin succession is diachronous, younger toward the craton; this is a hallmark of migrating foredeeps related to arc–passive margin collision. The flysch sequence coarsens and thickens upward and eastward, and the most proximal deposits are olisotostromal melanges that directly flank the thrust front and date thrust emplacement. The column on the right shows allochthonous deep-water deposits of the passive margin, where sedimentation was continuous and synorogenic flysch sedimentation commenced earlier than on the former platform. Ages of Events 1 through 4 here are a few million years older than in Newfoundland.

Author's personal copy



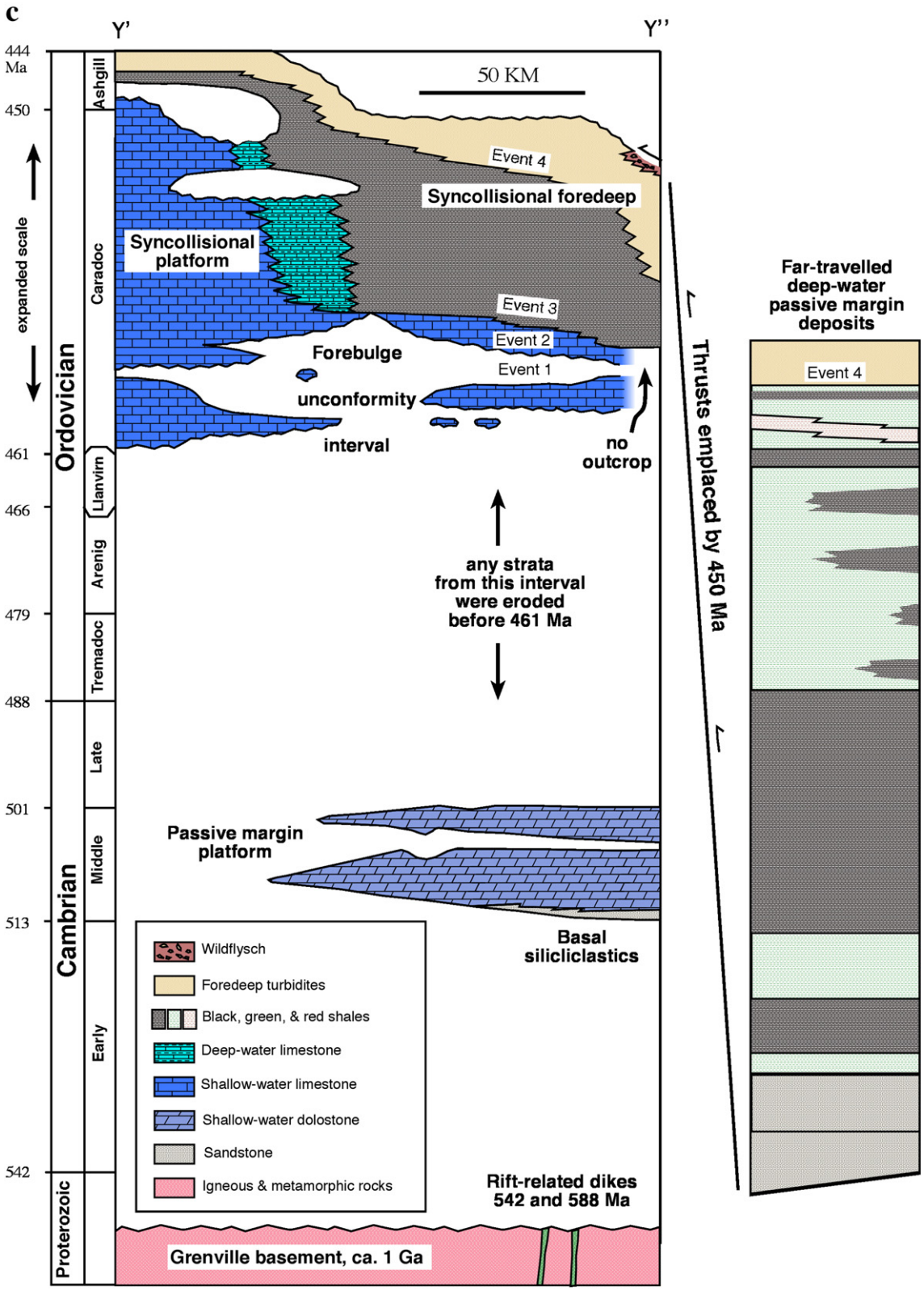


**Fig. 8** (*continued*).

p. 85). In light of the bracketing ages of 550 and 520 Ma, the rift-drift transition is here placed at ca. 540 Ma.[2] Paired with the shallow-water platform was an area of coeval, deep-water (slope-rise) deposition (Fig. 8b). These strata are important because they establish that the platform faced deep water for many tens of millions of years. The deep-water rocks occur in thrust sheets (allochthons in Fig. 8a) that were transported cratonward over age-equivalent platformal strata, which is a pattern commonly seen in ancient arc–passive margin collisions.

The collisional demise of the passive margin, known as the Taconic (or Taconian) orogeny, is recorded stratigraphically in both the original

[2] Similarly, Cawood et al. (2001) picked the age of the rift-drift transition at 540–535 Ma. Bond et al.'s (1984) much older age pick for the rift-drift transition in the Appalachians (600±25 Ma) was based on subsidence curves calibrated to a long-abandoned time scale.

Author's personal copy



deep-water and shallow-water realms. In the deep-water belt, impending collision was signaled by an influx of outboard-derived siliciclastic turbidites; as reviewed by Bradley (1989), this event took place in late Arenig time (Early Ordovician, ca. 478 Ma) in Newfoundland. Assuming that the most distal deep-water sections were deposited on oceanic crust, this transition would predate collision along that part of the margin. On the carbonate platform, the slightly younger event sequence was: (Event 1) epeirogenic uplift and emergence, (Event 2) renewed carbonate deposition, deepening upward into (Event 3) black shale deposition as the platform drowned, and then (Event 4) deposition of easterly-derived turbidites, which were shed from a submarine thrust belt that advanced from the east. Fig. 8c shows the diachronous nature of facies belts and the corresponding numbered events within the Taconic foreland, as revealed by a transect across northern New York (the equivalent strata in Newfoundland are under water). Event 1 has been attributed to uplift along a forebulge some 100–200 km landward of the orogenic front (*e.g.*, Knight et al., 1991). Events 2 and 3 were accompanied by margin-parallel normal faulting related to flexure of the passive-margin plate into the trench (Bradley and Kidd, 1991), perhaps augmented by whole-lithosphere extension caused by slab pull resisted by continental drag (Schoonmaker et al., 2005). Event 4 represents the Taconic foreland basin, which in Newfoundland comprises as much as nearly 2 km of deep-water turbidites ("flysch") (Hiscott, 1995). Platform drowning in Newfoundland took place in Llanvirn time (ca. 465 Ma; see Bradley, 1989, for original sources) and this is picked as the age of the passive margin-to-foreland-basin transition in Newfoundland. It should be stressed, however, that the time elapsed between Events 1 and 4 at any given location was only a few million years.[3]

The thrust allochthons that overrode the passive margin carried rift-, passive margin-, and foreland-basin deposits, all of them native to the Laurentian margin. Higher in the thrust stack are ophiolites, which unequivocally record the former existence of an ocean basin (Iapetus) to the east of the Laurentian margin. The ophiolites, including the very well-studied Bay of Islands ophiolite, have yielded U–Pb zircon ages from 508±5 to 484±5 Ma (see Williams et al., 1995 for original sources). Thus the ophiolites are substantially younger than the oldest seafloor (ca. 540 Ma) inferred to have lain immediately offshore Newfoundland as the oceanic part of the Laurentian plate. The Bay of Islands ophiolite is instead interpreted to have formed by seafloor spreading in a supra-subduction setting (*e.g.*, Jenner et al., 1991). Amphibolites from the metamorphic sole of the Bay of Islands ophiolite yielded a $^{40}Ar/^{39}Ar$ amphibole ages of 469±5 and 464±9 Ma (see Williams et al., 1995 for original sources); the metamorphic sole is interpreted as a relict of the paleo-subduction zone during or just before emplacement of the ophiolite onto the passive margin. In both Newfoundland and the northeastern United States, rocks of the former passive margin are now flanked to the east by Ordovician volcanic and plutonic rocks; arc magmatism in both areas spanned pre-, syn-, and immediately post-collisional times (Karabinos et al., 1998; Zagorevski et al., 2006). Waldron and van Staal (2001) presented evidence that the Ordovician arc that collided with Laurentia's passive margin was built on a ribbon microcontinent that had rifted away from Laurentia at ca. 540 Ma. In this model, the *outer* margin of this inferred ribbon microcontinent was a somewhat older passive margin, formed ca. 600–570 Ma (Waldron and van Staal, 2001).

The Taconic collision was accompanied by regional metamorphism of both basement and sedimentary cover of the Laurentian margin. In the northeastern United States, Taconic regional metamorphism reached kyanite grade and took place at 465±10 Ma ($^{40}Ar/^{39}Ar$ amphibole; Laird, in Drake et al., 1989). This age correlates remarkably well with the end date of the passive margin based on stratigraphic evidence. Along the Taconic suture, blueschist and eclogites have been discovered (Laird, in Drake et al., 1989), but only in a few small enclaves that would likely have been overlooked in a less thoroughly mapped region. These high-pressure rocks confirm the presence of a subduction zone during the Taconic collision.

The Cambrian–Ordovician of the Appalachians thus serves as a thoroughly studied example of a passive margin of moderate duration whose start date and end date are constrained by multiple lines of evidence. The age of the rift-drift transition is ca. 540 Ma, bracketed between isotopically dated rift-related igneous rocks and fossil-dated strata near the base of the drift sequence. Even without age control on the igneous rocks, the age of rifting would still be fairly well constrained by the youngest detrital zircons in rift sediments. The passive-margin to foreland-basin transition is even more tightly constrained at ca. 465 Ma, with age control provided by the oldest allochthonous flysch, the age of platform drowning, and metamorphic ages of passive-margin strata. These dates imply a lifespan of about 75 m.y.—relatively short by worldwide standards.

### 4.3. Verkhoyansk (eastern) margin of Siberia

Between ca. 1600 and 160 Ma, the east side of the Siberian craton (Fig. 9) was flanked by what I interpret as a succession of three passive margins (margins A56, A57, and A58). The first of these lasted longer than any other passive margin–from ca. 1600 to ca. 1010 Ma–and it also stands out as one of the few margins anywhere in the world during that interval. Two younger rift-drift episodes followed, from ca. 550 to 380 Ma and then from ca. 380 to 160 Ma. Each successive passive-margin episode masked any earlier history, and the rocks of each of the three margins were involved in the Mesozoic Verkhoyansk orogeny, which produced the world's widest fold–thrust belt.

The Proterozoic history is pieced together from widely separated outcrop areas along the eastern side of the Siberian craton: a northern Verkhoyansk sector that includes the Olenek Uplift and Kharalaukh Mountains and a southern sector that includes the Sette-Daban range (Fig. 9a). Riphean strata in both areas are the remnants of a miogeoclinal prism of carbonates and siliciclastics that thicken and are more distal to the east (Fig. 9b). Maximum thickness exceeds 5 km (Khudoley et al., 2001). The ca. 1600–1050 Ma miogeoclinal succession in the south (Uchur, Kerpyl, and Lakhanda Groups) depositionally overlies a rift (Ulkian succession; not in the line of section) containing volcanic rocks as young as 1676 Ma (Pisarevsky and Natapov, 2003). Pisarevsky and Natapov (2003) interpreted the mid-Proterozoic miogeocline as having formed along a passive margin, a view supported here.[4] They bracketed the rift-drift transition between ca. 1600 and 1480 Ma in the north. In the south, the rift-drift transition would fall between 1676 Ma, the youngest rift-related volcanic rocks, and 1520 Ma, the oldest K–Ar glauconitic sandstone age from the Uchur Group. For this compilation, I place the rift-drift transition at ca. 1600 Ma in both the north and south.

The new interpretation offered here is that the Mesoproterozoic passive margin was involved in a somewhat cryptic collision at ca. 1010 Ma. In the eastern Sette-Daban, the Lakhanda Group is depositionally overlain by the Uy Group, which consists of siliciclastics that were derived from both western (Siberian) and eastern sources (Khudoley et al., 2001) (Fig. 9b). These stand out as the first easterly-derived sediments in the Riphean succession, consistent with development or arrival of a new, outboard sediment source. Moreover, thicknesses and facies in the Uy Group are locally controlled by thrust faults (Khudoley and Guriev, 2003). The Uy Group has yielded detrital zircons as young as 1070±40 Ma, and is intruded by mafic sills that are as old as 1005 Ma (Rainbird et al., 1998). A ca. 400-m.y. gap in the

[3] Events 1–4 are diachronous both across strike and along the entire length of the Appalachians (Bradley, 1989); the age progression of platform drowning is interpreted as tracking plate convergence through time along an irregular margin.

[4] An alternative view is that the mid-Proterozoic miogeocline represents a sag sequence above a failed intracratonic rift (Khudoley et al., 2001).

Author's personal copy



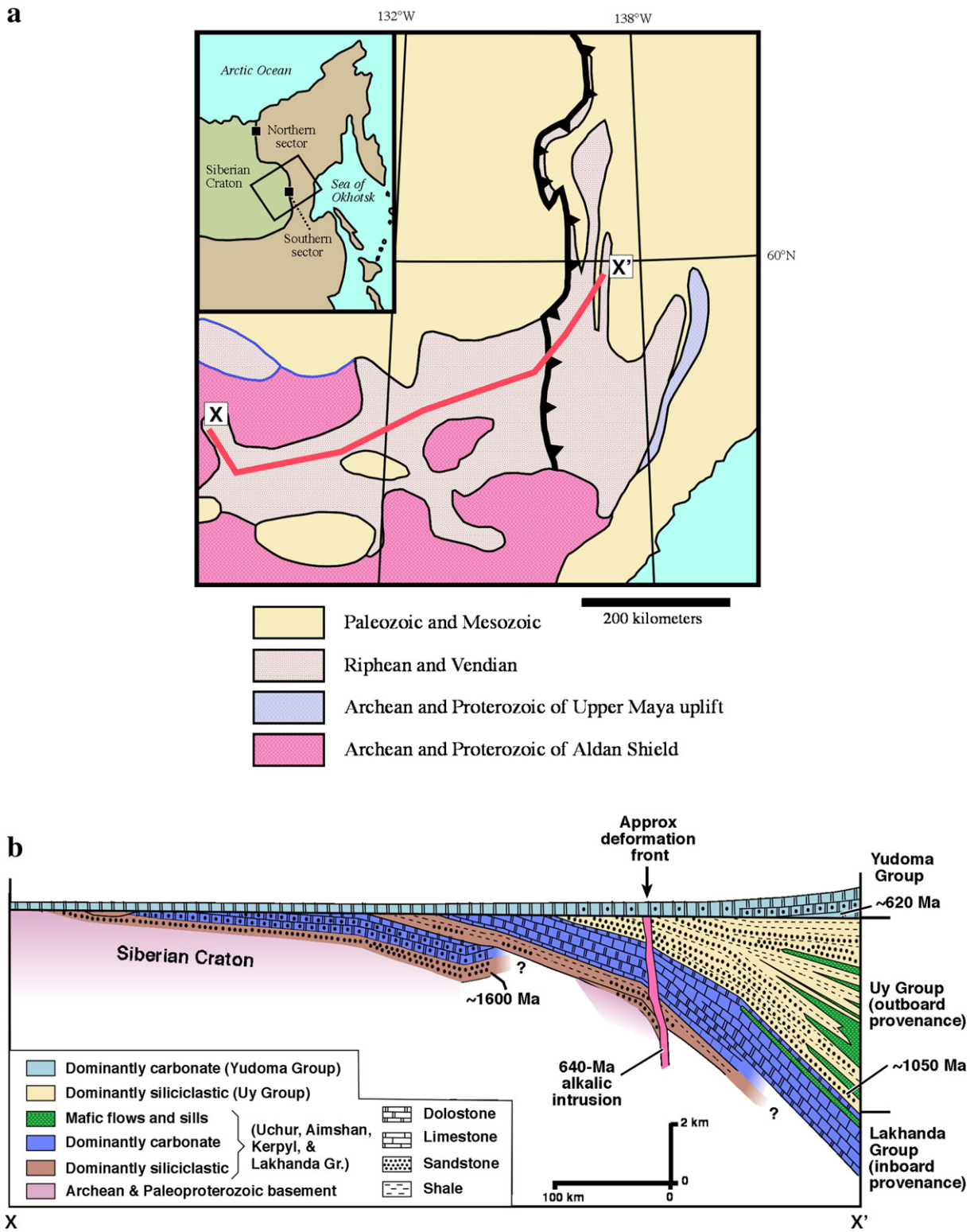


**Fig. 9.** (a) Generalized map of the Verkhoyansk region and eastern margin of Siberian craton, showing key features and localities mentioned in text, from Khudoley et al. (2001). (b) Stratigraphic reconstruction of Mesoproterozoic and Neoproterozoic rocks of the Siberian margin, modified from Khudoley et al. (2001). The Uy Group is here reinterpreted as a foreland-basin succession, related to orogenesis on the basin's eastern margin.

sedimentary record followed deposition of the Uy Group. The next younger rocks are Vendian strata beginning at ca. 620 Ma, which overlie an angular unconformity (Khudoley et al., 2001) that buries thrust faults. Together, these observations are consistent with the interpretation that the Uy Group is a foreland-basin succession and that the Mesoproterozoic phase of the Siberian craton's eastern passive margin ended with orogeny at ca. 1010 Ma. Whereas there is no known 1 Ga orogen east of the Sette-Daban ranges, such a feature would have departed when the next passive margin formed in the late Neoproterozoic, leaving only the foreland basin to record the collision.

An alternative view is that ca. 1000 Ma was a time of rifting (Khudoley and Guriev, 2003). Khudoley et al. (2001) interpreted an extensional tectonic setting for the Uy Group, presumably to account for mafic magmatism at the time. However, it is unclear why such

Author's personal copy



rifting would be followed by 400 million years of non-deposition rather than by thermal subsidence. Instead, I suggest that the mafic sills of the Uy Group were intruded in a foreland setting and not a rift—the same interpretation invoked by Hoffman (1987) for several Paleoproterozoic examples in Laurentia.

Adopting the passive margin and collision interpretation, the start date for the Mesoproterozoic margin would have been at ca. 1600 Ma and the end date would lie somewhere between 1070 and 1005 Ma, and probably close to the younger bracketing age. An end date of 1010 Ma would correspond to a lifespan of about 590 m.y.

Two additional phases of passive-margin evolution have been suggested along the eastern margin of the Siberian craton—Neoproterozoic to Devonian and Devonian to Jurassic. These are treated as separate passive margins (margin A57 and A58) because they appear to have formed by completely separate plate-tectonic events.

In northeastern Siberia, Pelechaty (1996) documented a Neoproterozoic carbonate succession that formed along the eastern, presumably passive margin to the Siberian craton. This >600-m-thick carbonate succession (Khorbosuanka Group) predates a rifting event at around the Neoproterozoic–Cambrian boundary related to a breakup event along the Siberian craton's *northern* (Taimyr) margin (Pelechaty, 1996) (margin A37). The base of the Khorbosuanka Group is ca. 550 Ma (Pelechaty et al., 1996), my pick for the age of the rift-drift transition. Khudoley and Guriev (2003, p. 34) cited evidence from subsidence analysis for multiple rifting events between 570 and 520 Ma, of unknown significance.

The Neoproterozoic to Devonian phase of passive-margin evolution ended not with collision, but with re-rifting. This final rifting event along the eastern margin of the Siberian craton has been interpreted to have involved the separation and departure of a Lomonosov-type continental sliver (Parfenov, 1991; Sengör and Natalin, 1996, p. 554). Rifting began in the Middle Devonian in the Sette-Daban zone and was widespread along the Siberian craton's eastern margin by the Late Devonian (Khudoley and Guriev, 2003). Khudoley and Guriev (2003) reviewed evidence for rifting in the Sette-Daban zone (*e.g.*, Famennian half-grabens filled with olistostromes). Lower Carboniferous limestones were uniformly deposited across the extended terrane and are interpreted to record post-rift thermal subsidence. The margin lasted until Late Jurassic when shortening began in the Verkhoyansk foldbelt (Sengör and Natalin, 1996, p. 556). Using ages of 380 Ma for the rift-drift transition and 160 for the passive margin to foreland-basin transition, the margin had a duration of about 220 m.y. Interestingly, these are quite close to the age picks for the Brookian margin of the Arctic Alaska terrane (margin A1).

### 4.4. Western margin of Kaapvaal craton

The Kaapvaal craton of South Africa (Fig. 10) is one of the world's oldest continental nuclei. Development of a Neoarchean passive margin along its western side (margin A77) is inferred both from outcrop data and from high-quality seismic-reflection profiles. This margin is highlighted here because it is one of the two oldest well-dated margins, and because one aspect of the tectonic interpretation offered here is new. The Ventersdorp Group (Fig. 10b), which consists of komatiites, continental flood basalts, chemical and clastic sedimentary rocks, and felsic volcanic rocks, has been interpreted to have been deposited during the initial rifting along this margin (Tinker et al., 2002). Zircon ages from the lower part of the Ventersdorp Group are 2709 ± 8 and 2714 ± 8 Ma (U–Pb; Armstrong et al., 1991). Rocks of the overlying Schmidtsdrif and Campbellrand Subgroups are interpreted to represent the thermal subsidence phase of passive-margin sedimentation. These strata were deposited in a westward-thickening, west-dipping sedimentary prism (Tinker et al., 2002) and consist mainly of shallow-marine carbonate rocks (Beukes, 1984, 1986). The base of the Schmidtsdrif Subgroup is reasonably well dated by a zircon age of 2642 ± 3 Ma (Pb-evaporation; Beukes cited in Tinker et al., 2002).

There is a lack of consensus as to what marks the demise of the passive margin. I suggest that the contact between the Campbellrand Subgroup and the overlying Asbestos Hills Subgroup (Fig. 10b) approximates this event. The Asbestos Hills Subgroup is a transgressive succession of iron formation (Kuruman and Griquatown Formations), and it is overlain by mudstone, siltstone, quartz wacke, and iron formation of the Koegas Subgroup. Hoffman (1987) interpreted similar successions (carbonates overlain by iron formation overlain by siliciclastics) along the Paleoproterozoic Wopmay (A6) and Animikie (A13) margins as recording the transition from passive margin to foreland basin. Applying a similar interpretation to the Kaapvaal margin, a fairly close age constraint for the transition is provided by a zircon age of 2465 ± 7 Ma (Armstrong et al., 1991) from the Kuruman Formation at the base of the Asbestos Hills Subgroup. This would imply that the final position of the deformation front lay approximately 100 km to the west of any present exposures. Ages of 2640 Ma for the rift-drift transition and 2470 Ma for the demise of the passive margin yield a lifespan of 170 m.y.

Other possibilities for the age of the demise bear mention. Tinker et al. (2002) inferred that rocks of the Asbesheuwels, and Koegas Subgroups were deposited in the same regime of thermal subsidence as the underlying Campbellrand Subgroup. Whereas Tinker et al. (2002) did not specifically comment on the demise of the passive margin, their interpretation would mean that the margin endured somewhat longer than is suggested here. A much longer lifespan (about 640 m.y.) is also conceivable, although less likely. The first significant shortening of rocks of the Campbellrand Subgroup took place at ca. 1900 Ma, after deposition of the Olifantshoek Supergroup (Fig. 10b), which consists of siliciclastic and some volcanic rocks dated at 1928 ± 4 (Pb–Pb zircon; Cornell et al., 1998). If this deformation records the end of the passive margin (a possibility raised by Maarten de Wit, oral communication, 2003), the western margin of the Kaapvaal craton would then rank as the longest-lived passive margin in Earth history.

## 5. Distribution of passive margins through time

The distribution of passive margins has been quite uneven through time (Fig. 5a). The peaks and valleys in the histogram serve to subdivide Earth history, the peaks representing times of relatively more continental dispersion, and the valleys times of continental aggregation. The passive-margin age distribution will be compared with various proposed supercontinents in Section 8.

The youngest group of margins in Fig. 5a extends from ca. 300 Ma to present. This includes all of the present-day passive margins as well as 13 ancient ones. The ancient margins alone show a young peak centered near 100 Ma, but this is purely an artifact that disappears when the modern passive margins of the same vintage are also included (Fig. 5a). The comparative abundance of modern passive margins is mainly due (1) to the ease with which they can be recognized, and (2) to the fact that the marine magnetic anomalies allow subdivision into sectors having different start dates. For example, the present-day eastern passive margin of Africa has been divided into five parts, but would probably end up being treated as a single margin if it was half a billion years old and now preserved in an orogenic belt.

Working back through time, the next feature of note is the pronounced late Paleozoic minimum (Fig. 5a). Only 5 passive margins can be counted during the time between 300 and 275 Ma, compared to 17 margins at the next older peak at ca. 530–505 Ma.

The next older age cluster of margins in Fig. 5a extends from 1000 to 300 Ma and has twin peaks at 530–505 Ma, and at 600–580 Ma. No single margin endured for this entire 700 m.y. interval. The younger portion of this interval includes the classic passive margins that formed on all sides of Laurentia near the Neoproterozoic–Cambrian boundary and were destroyed during subsequent collisions: the Franklinian (margin A5), Appalachian (margin A19a), Ouachita (margin A18), and northern and southern Cordilleran (margins A3 and A4). The earlier portion of this interval includes the Neoproterozoic margins of the West African craton (margins A67, A68, and A69), Sao Francisco craton (margins A63 and A64), Congo craton (margins A73 and A74), and

Author's personal copy



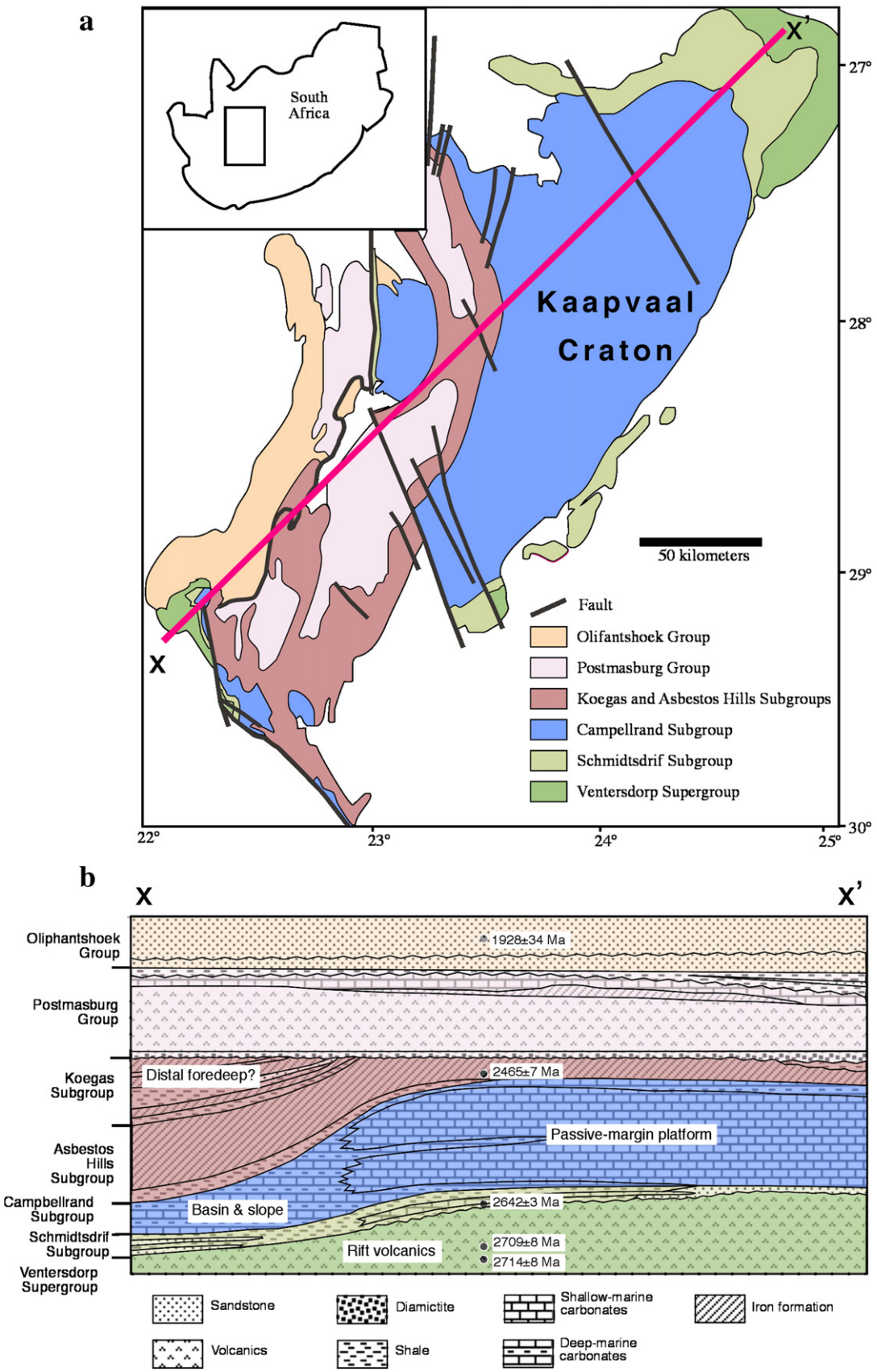


**Fig. 10.** (a) Generalized map of the western margin of the Kaapvaal craton, from Harding (2004). (b) Stratigraphic cross-section across the margin, from Harding (2004). Note that the siliciclastic Koegas Group is confined to areas of former off-shelf deposition, a pattern consistent with deposition in a foredeep related to a collision farther to the west.

Author's personal copy



Kalahari craton (margins A75 and A76), that were deformed in various Pan-African collision during the assembly of Gondwana.

Between 1740 and 1000 Ma, an interval approximately corresponding to Holland's (2006) "boring billion", passive margins were few in number, and from about 1740 to 1600 Ma, there appear to have been none at all. The Mesoproterozoic eastern margin of Siberia, which lasted some 590 m.y., has already been discussed. The western and southern margins of the Siberian craton (Yenisei—margin A38; and Baikal—margin A40) also fall in this age range, as do the eastern and northern margins of the Baltic craton (Uralian phase 1—margin A24; and Timan—margin A23). These five appear to be the longest-lived margins in Earth history, although they have poor quality rankings that reflect inadequate age controls and in a few cases, debatable tectonic interpretations.

The oldest well-defined peak in the passive-margin record is centered at 1900–1890 Ma and spans a range from ca. 2445 Ma to ca. 1740. Its apex corresponds to a time of continental dispersal and its end presumably corresponds to an aggregation of smaller continents into a larger one. Included in the 2445–1740 Ma group are excellent examples of passive margins bordering the Slave craton (Wopmay and Thelon; margins A6 and A7) and the Superior craton (Cape Smith-Trans-Hudson, and New Quebec; margins A14 and A15).

The oldest well-documented passive margins are the western margin of the Kaapvaal craton (margin A77, 2640–2470 Ma, discussed in Section 4.4), and the southwestern margin of the Pilbara craton (margin A83, 2685–2440 Ma). The Central Orogenic Belt of the North China craton may include an even older passive margin (margin A51, 2740–2530 Ma), but the tectonic interpretation is debatable. Together these define the oldest, minor "peak" in Fig. 5a. The oldest proposed passive margin, Steep Rock Lake (margin A10), existed sometime between 3000 and 2800 Ma but its tectonic interpretation is controversial and age controls are inadequate. If correctly interpreted by Kusky and Hudleston (1999), this margin would attest to something resembling a modern-style Wilson Cycle between 3000 and 2800 Ma.

No passive margins are known that are older than ca. 3000 Ma. This may be real, but could also involve difficulties in recognition, and lack of preservation. It would be difficult to correctly read the history of a short-lived rifted margin at the edge of a narrow Archean protocontinent that faced into a narrow ocean that opened and then immediately closed. Recycling of ancient crust could also contribute to the lack of pre-3000-Ma passive margins. Thus, the lack of margins before 3000 Ma in Fig. 5a is not definitive.

A key question is whether or not the irregular age distribution of passive margins as shown in Fig. 5a is real, or merely an artifact of an incomplete compilation. Comparisons with other secular trends, discussed in Section 9, suggest that the passive-margin age distribution is robust.

Fig. 5b shows the ages of rift-drift transitions for the 76 ancient margins in Group 1, plus all 75 modern ones. This plot reveals peaks at 500–550 and 600–650 Ma that are not obvious from Fig. 5a alone. A plot of rifting events by Condie (2002) shows a strong peak at 850–800 Ma that is barely evident in Fig. 5b; the difference between this plot and Condie's may lie in the fact that in the present study I picked the ages of rift-drift transitions, and was not too concerned with the full age range of prior rifting. Fig. 5c shows collision ages for the 81 ancient margins in Groups 1 and 2, with peaks at 300–400 and 550–600 Ma. This plot differs somewhat from a plot of collisions by Condie (2002), which shows 11 of them between 1300 and 1000 Ma, compared to just two in Fig. 5c. The discrepancy can be traced to Condie's inclusion of collisions that did not involve passive margins.

## 6. Lifespans of passive margins through time and implications for the tempo of plate tectonics

The overall *distribution* of passive margins through time shown in Fig. 5a is considered to be approximately correct. In contrast, corresponding plots of the *lifespans* of these margins (Fig. 11a and b) are significantly less reliable. Consider, for example, the Timanian margin of northern Baltica (margin A23). There is little doubt that it was a passive margin during the Neoproterozoic (*e.g.*, Roberts et al., 2004). The picked end date at 558 Ma seems quite reliable, as it is based on the U–Pb zircon age of a tuff from low in the foreland-basin section. On the other hand, the ca. 1000 Ma start date is extrapolated from Baltica's southern Uralian margin (margin A24), which appears to have been continuous with the Timanian margin. The Uralian margin's start date itself is equivocal and approximate. Even if the exact start date was off by 100 m.y., the Timanian margin would still contribute to the same overall peak in Fig. 5a, albeit in a different number of bins. But 100 m.y. would make a big difference to the lifespan of the margin (Fig. 11).

Keeping these caveats in mind, the lifespans of the 76 ancient passive margins in Group 1 are shown in Figs. 11 and 12. They range from about 20 to about 590 m.y. The mean lifespan of all ancient margins is 181 m.y. Subdividing the margins according to the natural age groupings suggested by Fig. 5a: (1) Seventeen passive margins that formed during the Neoarchean to Paleoproterozoic (2800–1600 Ma) have a range of estimated lifespans from 20 to 370 m.y. Their mean lifespan is a surprisingly long 186 m.y. (2) Only six margins began in the Mesoproterozoic (1599–1000 Ma); these have lifespans that range from 55 to 590 m.y. and a mean lifespan of 394 m.y. (3) Twenty-five margins with start dates in the Neoproterozoic (999–542 Ma) have lifespans ranging from 25 to 370 m.y. and a mean lifespan of 180 m.y. (4) Fifteen margins that began in the early and middle Paleozoic (Cambrian to Carboniferous) have a range of lifespans from 57 to 220 m.y. and a mean of 137 m.y. (5) Thirteen ancient margins that began in the Late Permian or thereafter have a range of lifespans of 23 to 219 m.y. and a mean of 130 m.y. (6) Finally, as noted before, the mean (partial) age of the 75 modern margins is 104 Ma and the range is 5 to 180 m.y.

At face value, the data plotted in Figs. 11 and 12 suggest that passive margins generally had longer lifespans in the Precambrian than in the Phanerozoic. This conclusion needs to be balanced against the fact that the lifespans of the modern margins are still incomplete. The Atlantic margin of West Africa, for example, is already about 170 million years old today, and it will endure for many tens of millions of years to come, until it finally collides with the Caribbean arc. A more apt comparison can be made by eliminating the modern margins, and the ancient margins of about the same vintage (*i.e.*, those that formed from Late Permian onward.) Applying this filter, the 15 Phanerozoic margins with Cambrian to Carboniferous start dates had a mean lifespan of 135 m.y., compared to the 47 margins with Precambrian start dates, which had a far longer mean lifespan of 206 m.y.

When beginning the present study, I anticipated the opposite result—shorter lifespans in the Precambrian. The shorter-lifespan hypothesis had been posed by Hoffman and Bowring (1984) and later by Grotzinger and Ingersoll (1992), as a corollary of the hypothesis that the hotter Earth of the Precambrian dissipated its heat via smaller, faster plates. Given the decline in global radiogenic heat production through Earth history, it had long been suggested that the global rate of seafloor production would have been higher in the Precambrian than the Phanerozoic (*e.g.*, Burke et al., 1976; Nisbet and Fowler, 1983; Hargraves, 1986; Pollack, 1997). At 2500 Ma, heat production would have been about two times the present value, and as recently as 1500 Ma, it would still have been about 1.5 times the present value. But heat production is not the same as heat loss. Recent thermal modeling by Korenaga (2006) has provided a strong theoretical case for an early Earth characterized by *sluggish* plate tectonics. For supporting geologic evidence, Korenaga (2006) cited the perceived slowdown in the supercontinent cycle over time. As discussd in Section 8, published supercontinent scenarios are debatable. Results of the present study provide stronger corroboration of Korenaga's (2006) findings: on average, Wilson Cycles were slower, not faster, in the Precambrian.

Author's personal copy



## 7. Secular changes in the geology of arc–passive margin collision

Collisions between arcs and passive margins appear to have been happening since the Neoarchean. Whereas many of the older examples are problematic owing to polyphase orogeny and destruction of the sedimentary record, a few are comparable in all important respects to Phanerozoic arc–passive margin collisions. The classic Proterozoic example is the Wopmay orogen along the western margin of the Slave craton (margin A6) (Hoffman, 1980).

### *7.1. High-pressure, low-temperature metamorphism*

Some secular changes, however, are apparent. High-pressure, low-temperature metamorphic rocks form in oceanic subduction zones such as the Franciscan Complex of California, but also in collisional orogens where passive continental margins are partly subducted (Maruyama et al., 1996). Blueschist- and (or) eclogite-facies metamorphic rocks were noted in 17 of the arc–passive margin collisional orogens in the present compilation (Fig. 13a and Table 2). Among the oldest examples is the Neoproterozoic Dahomeyide orogen on the eastern side of the West African craton (Jahn et al., 2001) (margin A69). None of the arc–passive margin collisions older than ca. 625 Ma is known to have produced blueschists that are now exposed at the surface, whereas roughly half of the collisions since that time did. The long-standing explanation for the lack of old blueschists is that steeper geotherms on the hotter Earth precluded their formation (Maruyama et al., 1996 and references therein).

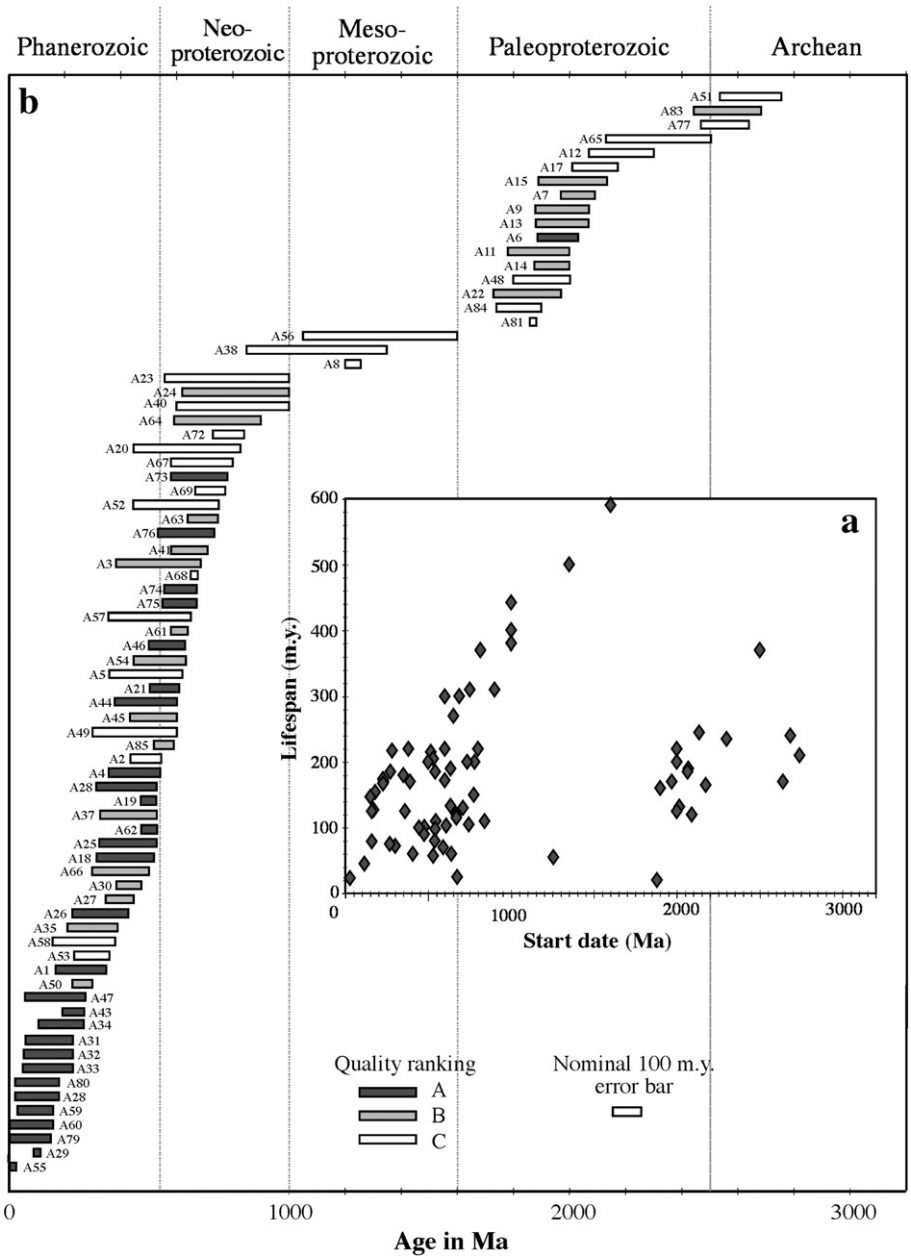


**Fig. 11.** Lifespans of ancient passive margins displayed in two ways, from data in Table 2. (a) Lifespan plotted against start date, showing the age of each margin at the time of its demise. Note the apparent long-term secular trend toward shorter lifespans over time and the hint of two cycles of declining lifespan. (b) Each margin is plotted as a horizontal bar extending from the start date to the end date; longer bars mean longer lifespans. Bars are arranged chronologically by start date, and keyed by color according to quality ranking. Even the longest-lived passive margins are ephemeral features when viewed at the timescale of Earth history.

Author's personal copy



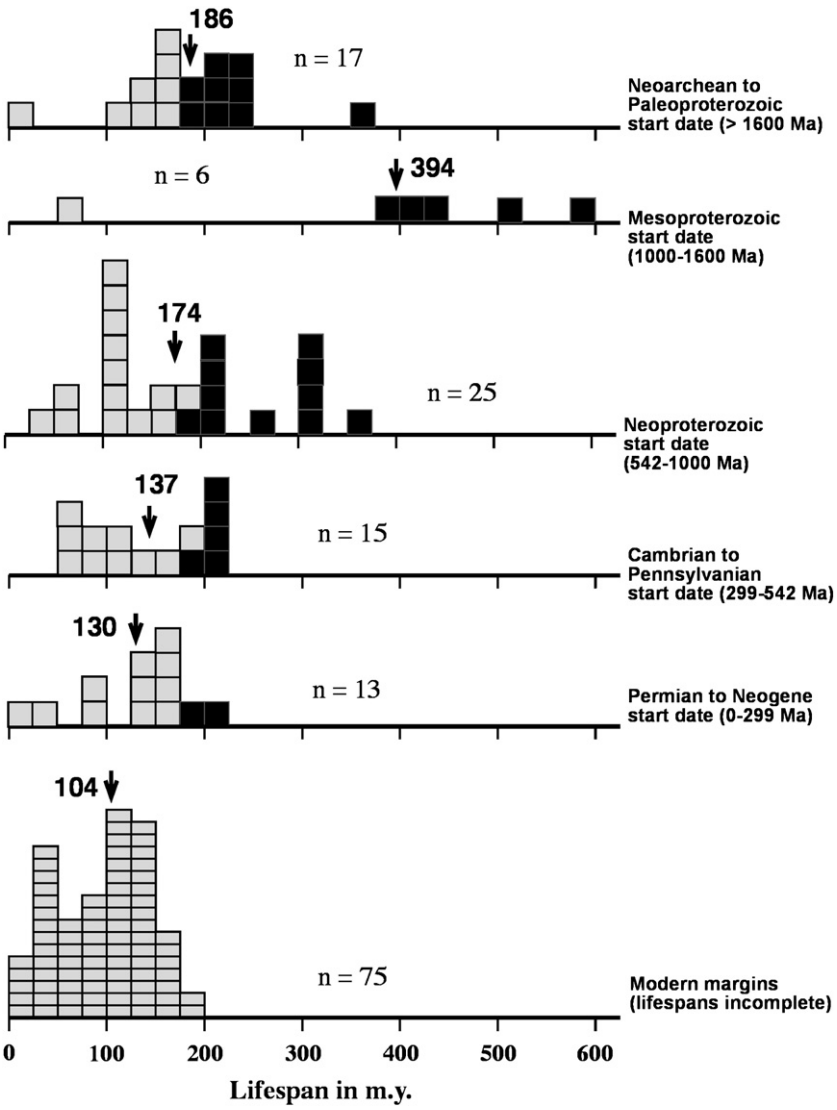


**Fig. 12.** Histograms showing lifespans of passive margins, grouped according to the natural divisions of geologic time suggested by Fig. 5a. The mean lifespan for each age group is indicated by an arrow and number in m.y. The eighteen longest-lived margins all had start dates in the Archean or Proterozoic. Black bins represent margins that lasted longer than the oldest modern margin, *i.e.*, 180 m.y. or older.

### *7.2. Foredeep magmatism*

Although collisional foredeeps are not generally recognized as sites of magmatic activity, the phenomenon is more common than is generally appreciated. Synorogenic foredeep magmatism was first noticed and discussed at length by Hoffman (1987), who identified predominantly mafic magmatism in the forelands of six Paleoproterozoic collisional orogens in Canada. Two of the best-documented of these are at the margins of the Slave and Superior cratons (*e.g.*, Wopmay and Penokean forelands; margins A6 and A13). In the Penokean foreland, mostly mafic submarine volcanic rocks are interbedded with euxinic, deep-water shales and turbidites (Hoffman, 1987). In the Wopmay foreland, mafic sills are intruded into, and folded with, flysch and molasse facies (Hoffman, 1987).

The present compilation has unearthed some additional examples of foredeep magmatism, bringing the number of recognized instances to fifteen (Fig. 13b and Table 2). The oldest is along the Pilbara craton's southwestern margin (margin A83), where the Woongarra Volcanics (ca. 2491 Ma) were deposited immediately before the Boolgeeda Iron Formation, which is thought to have been deposited on a forebulge (Martin et al., 2000). As Hoffman (1987) recognized, the youngest instance of foredeep magmatism is the Penghu Islands volcanic field in the foreland of the Neogene Taiwan collision (margin A55). In addition, it seems likely that many instances of foredeep magmatism have been overlooked, because mafic magmatism has often been interpreted as *prima facie* evidence for rifting.

Although at first it seemed to be mainly a Proterozoic phenomenon, the incidence of foredeep magmatism does not show a clear secular trend (Fig. 13b). Proterozoic occurrences do, however, seem to be larger. The general problem of magma genesis in or below the lower (foreland) plate of collision zones has not been systematically tackled, and it remains an important problem nearly two decades after Hoffman's (1987) seminal paper.

## 8. Comparisons with postulated supercontinents

"*Supercontinents* are assemblies of all or nearly all the Earth's continental blocks" (Rogers and Santosh, 2003). A *supercraton* (Bleeker, 2003) is an assembly of several continents, but not all of

Author's personal copy



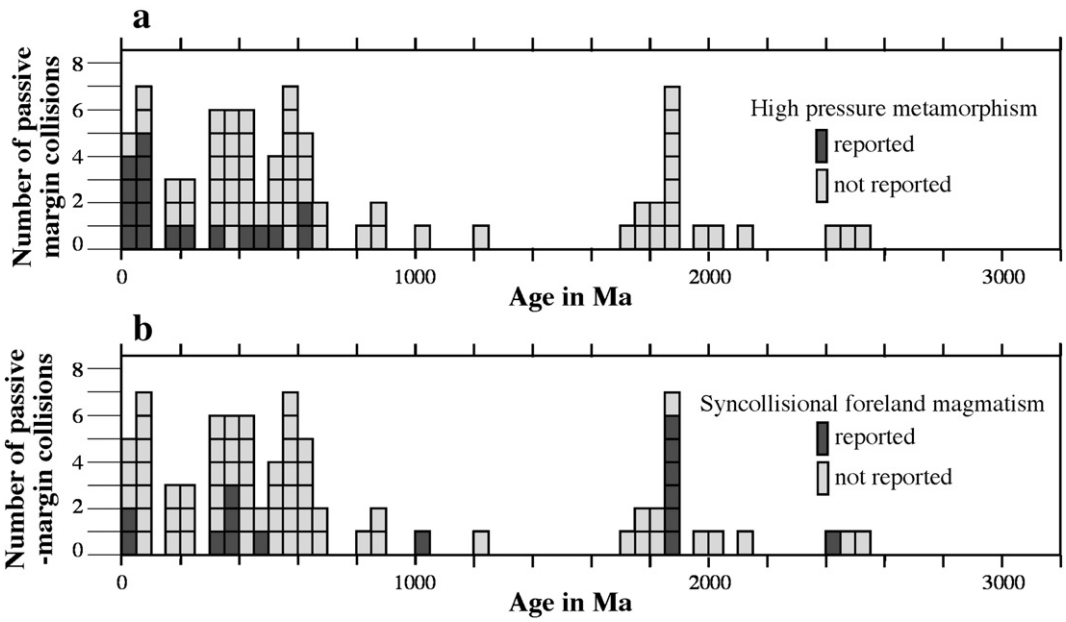


**Fig. 13.** Histograms showing end dates of passive margins, highlighting instances of (a) syncollisional blueschist metamorphism, and (b) syncollisional foredeep magmatism. From data in Table 2.

them. From first principles, passive margins should relate to the supercontinent cycle as follows: (1) the assembly of a supercontinent should correspond to a decrease in the world's population of passive margins; (2) during the tenure of a supercontinent, relatively few passive margins are to be expected (because the global length of continental margins of all sorts would be reduced); and (3) during supercontinent breakup, passive margins should increase in number. Fig. 14e shows the age distribution of hypothesized supercontinents and other large continental groupings, modified from Rogers and Santosh (2003). Of the variables that are compared with the passive margin age distribution in Fig. 14, supercontinents are not as independent, because various ones have been postulated, in part, on the basis of passive margins. A comparison between Fig. 14a and e shows many of the expected correspondences but also discrepancies for which some tentative explanations are offered.

### 8.1. Pangea

The most striking correlation between Fig. 14a and e involves Pangea, which formed and broke up during that part of Earth history having by far the clearest geologic record. The maximum of extent of Pangea (ca. 310 to ca. 180 Ma; from reconstructions in Scotese, 2004) coincides with the low in the passive-margin age distribution at 300 to 275 Ma. The increase in passive margins since then clearly equates to the breakup of Pangea. Likewise, the decline in the number of passive margins from ca. 500 to ca. 350 Ma coincides with the assembly of Pangea. The existence of Pangea is unassailable, and the correlation with the passive-margin record is excellent. The supercontinent record before Pangea is contentious and correlations with the passive-margin record are likewise uneven.

### 8.2. Pannotia

A reconstruction by Dalziel (1997) at ca. 545 Ma shows a single Pannotia supercontinent featuring East Gondwana,[5] West Gondawana, Laurentia, Baltica, and Siberia. Dalziel (1997) suggested that this supercontinent was distinct from Rodinia (see next paragraph) and was rather short lived (ca. 600 to 540 Ma). The number of passive margins steadily climbed starting at 1000 Ma, peaked at 600–590 Ma (19 margins), declined to a minor low at 555–545 Ma (13 margins), and peaked again at 530–520 Ma (18 margins) (Figs. 5a and 14a). Thus, the time of Pannotia as proposed by Dalziel (1997) includes the time when passive margins were at their most abundant, which clearly does not follow the Pangean analogue. If anything, the passive-margin record would squeeze Pannotia into a very brief interval from 555 to 545 Ma. But even this is unsatisfactory: some Neoproterozoic passive margins were meeting their ends in Gondwana (*e.g.*, northern and western margins of the Kalahari craton, A75 and A76) well after two of the passive margins surrounding Laurentia had already gotten started (margins A3 and A5). Thus, Pannotia was never a supercontinent according to the strict definition.

### 8.3. Rodinia

A broad consensus supports the existence during the early Neoproterozoic of a supercontinent, which has been called Rodinia by most researchers, or Paleopangaea by Piper (2000). The most convincing evidence for such a supercontinent would be a bomb-proof reconstruction like that for Pangea. Instead, several very different Rodinia reconstructions have been proposed (*cf.* Hoffman, 1991A; Dalziel 1997; Karlstrom et al., 1999; Piper, 2000), which share the assumption that all the world's continents were gathered into a single supercontinent. Condie (2003) summarized Rodinia's timing as follows: assembly between 1300 and 950 Ma, supercontinent at 950 to 850 Ma, and breakup between 850 and 600 Ma. Similarly, Rogers and Santosh (2003) gave the age of Rodinia as ca. 1100 to 800 Ma. The passive-margin record agrees broadly with the concept of a late Mesoproterozoic Rodinia supercontinent that broke up during the Neoproterozoic: a time of few margins at ca. 1200 to 1050 Ma was followed by an increase from ca. 1050 to 600 Ma. On the other hand, the general scarcity of passive margins during the Mesoproterozoic, when Rodinia was supposedly being assembled, cannot be readily explained by analogy with the Pangea case.

[5] Gondwana has been treated as a supercontinent by some researchers but in fact it only contained about half the world's continental area.

Author's personal copy



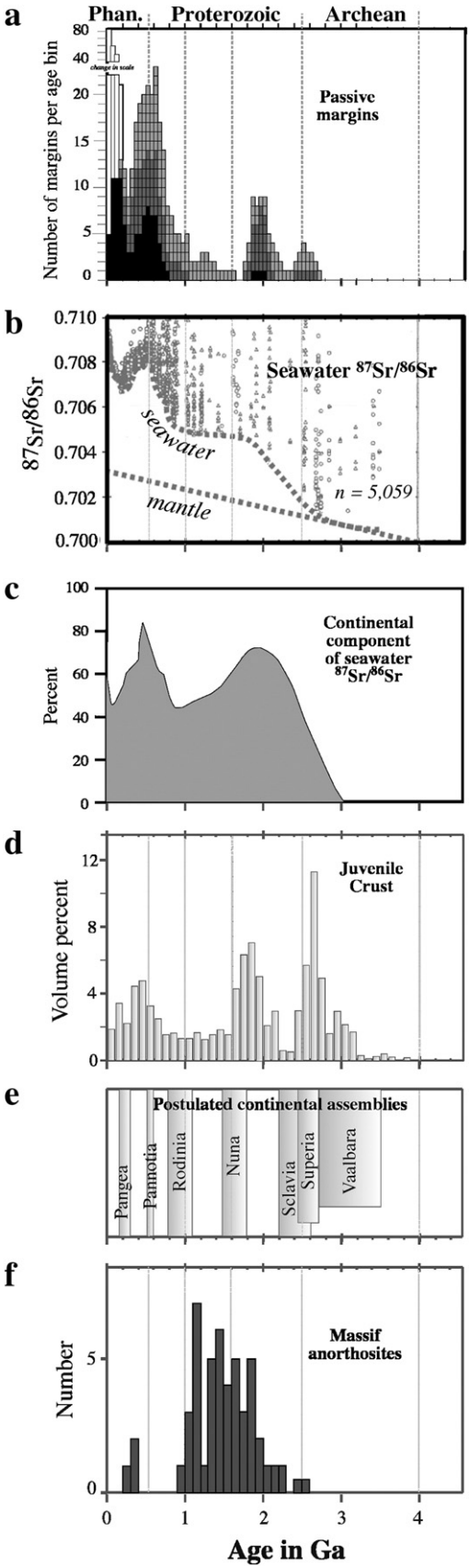


**Fig. 14.** Comparisons between geologic time series: (a) distribution of passive margins from Fig. 5a. (b) Seawater $^{87}Sr/^{86}Sr$, from Veizer and McKenzie (2003). (c) Normalized seawater $^{87}Sr/^{86}Sr$, showing just the continental contribution, from Shields (2007). (d) Juvenile crust, from Condie (2005). (e) Supercontinents, from sources cited in Section 8. (f) Massif anorthosites, adapted from data tabulated by Ashwal (1993). Note the remarkable positive correlation between the passive-margin distribution and the normalized strontium curve, and the negative correlation between the passive-margin and anorthosite distributions.

### 8.4. Nuna

An older supercontinent, referred to as Nuna (Hoffman, 1997) or later as Columbia (Rogers and Santosh, 2002), is proposed to have existed long before Rodinia, during the late Paleoproterozoic. There is ample evidence that a number of preexisting smaller cratons came together during this interval (*e.g.*, Hoffman, 1991A), but the case that almost all the world's continents were gathered into a *single* supercontinent is not compelling. The issue remains to be settled because the various proposed configurations are quite different (*cf.* Hoffman, 1997; Rogers and Santosh, 2003; Zhao et al., 2004). Hoffman (1997) presented a strong case that Laurentia, Greenland, and Baltica had come together by 1800 Ma. According to Rogers and Santosh (2003), what they referred to as Columbia came together ca. 1800 Ma and broke apart ca. 1500 Ma. According to Zhao et al. (2004), this supercontinent came together (in a very different configuration) by a series of collisions from 2100 to 1800 Ma, grew by subduction–accretion until ca. 1300 Ma, and then broke up, to reform soon thereafter as Rodinia. The passive-margin record is broadly consistent with the idea of a late Paleoproterozoic supercontinent, but not with the timing of breakup in either the Rogers and Santosh (2003) or the Zhao et al. (2004) scenarios. An abundance of passive margins between ca. 1850 and 2050 Ma was followed by a precipitous drop between ca. 1850 and 1750 (Fig. 5a). The drop corresponds to the postulated assembly of Nuna. But the passive-margin record summarized in Fig. 5a provides no independent confirmation of the idea that during the Mesoproterozoic, a supercontinent broke up and then reformed into Rodinia.

### 8.5. Sclavia, Superia, and Vaalbara

These are Archean continental groupings, or supercratons, that are based on a comprehensive global assessment by Bleeker (2003). Sclavia includes Canada's Slave craton and various other cratons that rifted away from it during the Paleoproterozoic; it is proposed to have existed from ca. 2600 to 2200 Ma (Bleeker, 2003). The slightly older Superia includes Canada's Superior craton plus various objects that rifted from it during the Paleoproterozoic; it is proposed to have existed from ca. 2700 to 2450 Ma (Bleeker, 2003). Vaalbara includes the Kapvaal and Pilbara cratons and is propose to have been together from ca. 3470 to ca. 2700 Ma (Bleeker, 2003). None of these meet the strict definition of a supercontinent. The passive-margin record is consistent with all three, subject to minor age adjustments discussed below.

### 8.6. Proposed scenario

The passive-margin record suggests a somewhat different history of continental aggregation and dispersal than has been previously published. Except for Pangea, none of these groupings can be definitively labeled supercontinents because there is no way to confirm that any of them contained almost all of the world's continental crust in a single entity. Indeed, casual usage of the term “supercontinent” provides circular support for the concept of a supercontinent cycle. Semantics aside, the passive margins clearly confirm that times of continental dispersion have alternated with times of continental aggregation during at least the latter half of Earth history.

Author's personal copy



The patchy record of passive margins in the Archean is consistent with Bleeker's (2003) scenario for three supercratons, subject to minor changes in breakup ages as per Table 2: Vaalbara from ca. 3470 to ca. 2685, Superia from ca. 2700 to ca. 2300, and Sclavia from ca. 2600 to ca. 2090 Ma. Breakup of these supercratons during the first half of the Paleoproterozoic led to a peak in the population of passive margins at ca. 1900 Ma. One by one, each of these margins collided with something, leaving no passive margins at all from ca. 1740 to ca. 1600 Ma. The passive-margin record is consistent with the purported coalescence of Nuna by this time, with Laurentia at its core—but whether or not Nuna met the strict definition of a supercontinent, or was merely a supercraton, remains to be demonstrated. This allows the possibility that Nuna and at least one other supercraton formed around the end of the Paleoproterozoic.

The passive-margin record provides little support for previous hypotheses of wholesale breakup of a single supercontinent during the Mesoproterozoic, whose pieces came back together at ca. 1000 Ma in a new configuration called Rodinia. Instead, I suggest that Nuna grew by lateral accretion of juvenile arcs during the Mesoproterozoic (*e.g.*, Karlstrom et al., 2001), and that two or more supercratons came together during a series of Grenvillian collisions (ca. 1190–980 Ma; Rivers, 1997). This grouping equates to the supercontinent Rodinia of previous workers—but whether or not *it* was truly a single entity remains debatable, because the fit of the Rodinia continents remains equivocal.

Rodinia began to breakup even as it was supposedly forming: the first Uralian, Timanide, and Baikal margins (A24, A23, and A40) all formed at ca. 1000 Ma, while in eastern Laurentia, Grenvillian collision was nearing its end. Many breakups followed during the early to mid-Neoproterozoic, and the population of passive margins reached its maximum in the ancient record at 610–590 Ma. As discussed above, the hypothesized supercontinent Pannotia seems to have been an ephemeral grouping of some but not all of the continents. A number of passive margins began before and ended after the putative 600–540 Ma tenure of Pannotia (Fig. 11b). Almost all of the continents finally had come together by about 300 Ma to form Pangea, which broke up starting 180 Ma. Even Pangea, the archetypal supercontinent, did not quite contain all the world's continents (*e.g.*, Arctic Alaska microcontinent).

### 8.7. Implications for continental reconstructions

With a few straightforward exceptions,[6] age assignments for the passive margins in the present study were independent of continental reconstructions in the published literature. The data summarized in Table 2 thus can be used to evaluate and refine continental reconstructions. Conjugate margins that have come to be separated by the opening of an Atlantic-type ocean should come in matched pairs, like the present-day margins of eastern North America and western Africa. Where is the passive margin that matched the Innuitian margin of Arctic North America (margin A5)? The missing conjugate margin should have a start date of about 620 Ma, as well as basement geology consistent with having broken away from the Canadian Arctic. The matching margin might flank a craton, but the possibility cannot be ignored that it formed along a ribbon microcontinent—the sort of object that is not as widely recognized or well publicized, but just as important for this kind of research.

[6] The start date of the Jurassic margin of Venezuela (margin A60) was borrowed from the start date of its supposedly conjugate margin, in Cuba. Likewise, the start date for the northern margin of the Kalhari craton (A75) was borrowed from the supposedly conjugate southern margin of the Congo craton (A74). The start- and end dates for the now-dismembered Neoproterozoic to Paleozoic East Greenland-Svalbard margin (margin A20a and b) were inferred by combining evidence from both. The start- and end dates for the now-dismembered Cambrian to Pennsylvanian Sierra de la Ventana-Cape-Ellsworth margin (margin A66a, b, and c) were inferred by combining evidence from each.

## 9. Comparisons with other aspects of Earth history

### 9.1. Isotopic composition of seawater strontium

The age distribution of passive margins shows a striking correlation with fluctuations in the isotopic composition of $^{87}Sr/^{86}Sr$ in seawater (*cf.* Fig. 14a, b, and c). Overall, the global $^{87}Sr/^{86}Sr$ ratio has increased through geologic time owing to the inexorable decay of the world's initial allotment of $^{87}Rb$ to $^{87}Sr$. Fluctuations in the $^{87}Sr/^{86}Sr$ isotopic ratio of seawater track the shifting balance between sources of primitive mantle strontium (low $^{87}Sr/^{86}Sr$), which mostly enters seawater via hydothermal circulation at mid-ocean ridges, and evolved strontium (high $^{87}Sr/^{86}Sr$), which mostly enters the sea at continental margins (see review by Veizer and McKenzie, 2003, and references therein). The curve in Fig. 14b shows the raw data (from Veizer and McKenzie, 2003); the curve in Fig. 14c (from Shields, 2007) is normalized so as to show just the continental contribution to seawater Sr. The highs at 1900–1890, 610–520, and 150–0 Ma in the passive-margin distribution have close counterparts in the normalized strontium curve. The lows at >2750 and 300–275 Ma also are reflected in the strontium curve, but slightly offset. Between the two curves, there is only one significant mismatch: both show broad mid-Proterozoic lows, but they are skewed, with the minimum being centered at about 1740–1600 Ma for passive margins, compared to 1000–900 Ma for strontium. This discrepancy may indeed be real, but it should be noted that all but one of the passive margins that formed between 1700 and 1000 Ma have quality rankings of C, and moreover, that the strontium data are sparse (Fig. 14b). Regardless of this one discrepancy, the overall similarity between the two time series is striking—especially when one remembers how utterly independent the datasets are: the strontium curve is based on thousands of isotopic analyses of calcium carbonate, whereas the passive-margin curve is a compilation of tectonic interpretations of 76 orogenic belts. The broad form of the passive-margin age distribution appears to be correct and cannot be written off to poor preservation or an inadequate compilation.

Why should such a correlation exist? It would appear that classic Wilson Cycles involving the formation and destruction of passive margins are an effective way to involve large volumes of old continental basement in the sedimentary cycle (Richter et al., 1992). In contrast, plate interactions involving only isotopically primitive rocks (*e.g.*, oceanic crust, intraoceanic arcs, and recently formed continental crust) would contribute scant evolved strontium to the sea, no matter the intensity of orogeny, the extent of synorogenic exhumation, or the tempo of plate tectonics. A contributing factor may be the size of continents (Halverson et al., 2007): a single supercontinent with an arid interior would probably transmit less radiogenic strontium to the sea than would an equal area of smaller, dispersed continents having a greater perimeter. Significantly, neither the rift-drift-transition histogram (Fig. 5b) nor the arc–passive margin collision histogram (Fig. 5c) is as good a match for the normalized strontium curve (Fig. 14c) as the overall passive-margin histogram (Figs. 5a and 14a).

### 9.2. Juvenile crust

The age distribution of juvenile continental crust shows prominent maxima at ca. 2700–2600, 1900–1800, and 500–300 Ma, and minima before 3200 Ma, at 2400–2200 Ma, at 1700–700 Ma, and at 300–200 Ma (Fig. 14d) (Condie, 2005). Comparison with the passive-margin record (Fig. 14a) shows a fairly good correspondence at first order, except for the last hundred million years.

### 9.3. Massif anorthosites

The age distributions of passive margins and massif anorthosites (*cf.* Fig. 14a and f) show an extraordinary negative correlation. The

Author's personal copy



massif anorthosite distribution, which was constructed from a tabulation by Ashwal (1993), shows a broad peak between 2.0 and 1.0 Ga that coincides with the broad Mesoproterozoic low in the passive-margin distribution (the "boring billion" of Holland, 2006). Hoffman (1989) suggested that the anorthosite pulse was a consequence of thermal blanketing of the mantle by a large, stationary Laurentian continent (which would now be referred to as Nuna, or Columbia). The passive-margin record is consistent with this idea.

## 10. Less common fates of passive margins

As previously noted, the ancient passive margins in this synthesis had one of three fates: (1) collision, (2) re-rifting, and (3) conversion to a convergent margin. Here I elaborate on the last two.

### 10.1. Re-rifting

Re-rifting (Sengör, 2004) involves the departure of a ribbon continent or microcontinent from an existing passive margin. For this to happen, a new spreading ridge must break through near the ocean–continent boundary. Re-rifting is a more common process than is generally appreciated. The best young example is the Barents Shelf of the Arctic, which already was a passive margin in the Cretaceous when a new spreading center developed near the old ocean–continent boundary, leading to the separation of the Lomonosov ribbon microcontinent (*e.g.*, Kristoffersen, 1990). Ribbon microcontinents are believed to have rifted from the eastern Laurentian passive margin in the Neoproterozoic to Cambrian (margin A19a; Waldron and van Staal, 2001), and from the eastern passive margin of Siberia in the Devonian (margin A57; Parfenov, 1991; Sengör and Natalin, 1996; p. 554). The Tethyan realm abounds with passive margins that appear to have formed by the breakaway of ribbon microcontinents, which left the Gondwana margin on the south, and drifted north to collide with Eurasia (Sengör et al., 1988; Stampfli et al., 1991).

### 10.2. Conversion to a convergent margin

Direct conversion of a passive to a convergent margin (Fig. 1b) is rare indeed, as Burke et al. (1984) first showed and the present work confirms. The notion that this is commonplace dates at least as far back as Dewey and Bird (1970) in their pioneering paper that tied plate tectonics to orogenic geology. The present compilation shows that a passive margin can attain great age *without* converting directly to an Andean-type margin; eleven of them lasted at least 300 m.y.

That it is *possible* for a passive margin to convert directly to a convergent margin is demonstrated, however, by the history of the northern margin of Iberia, facing the Bay of Biscay (margin A29). It formed in the Early Cretaceous (ca. 115 Ma) when Iberia broke away from Europe. In the Late Cretaceous (late Senonian, ca. 70 Ma), convergence across the ocean–continent boundary began, and an accretionary wedge formed (Vergés and García-Senz, 2001). Significantly, a full-fledged, enduring subduction zone never did form, as there is no magmatic arc and the margin eventually lapsed into inactivity.[7] The Iberian passive margin thus lasted a mere 45 m.y., making it one of the shortest-lived ones in the entire dataset. When this passive margin failed in compression, it was not because it had grown old.

The first proposed instance of conversion from passive margin to convergent margin was the Appalachian margin during the Ordovician (Bird and Dewey, 1970) (margin A19a). This scenario for the Taconic orogeny was quickly abandoned after Stevens (1970) advanced the more compelling arc–passive margin collision interpretation that is described in Section 4.2. The northern part of the Canadian Cordilleran passive margin (margin A3) is interpreted here as having collided with an arc during the Devonian, but an alternative (implied, for example, by Nelson et al., 2002) is that it converted to a convergent margin without first colliding with something. Direct conversion from passive- to convergent margin has been proposed for three other margins that weren't included in the present synthesis, for want of detailed information. The early Paleozoic Gondwanan margin of Chile is proposed to have converted directly from a passive margin to a convergent one during the Ordovician (Bahlburg and Hervé, 1997). The North Afghan platform has been interpreted as the site of an Ordovician? to Early Devonian passive margin that developed into an arc in Late Devonian and Mississippian time, apparently without a collision in between (Brookfield and Hashmat, 2001). A similar history has been proposed for the southern margin of the Iranian plate during the Late Triassic (Sheikholeslami et al., 2008). A geologic model for this process, based on well-documented case studies, would be a valuable contribution.

## 11. Summary

1. Passive margins have existed somewhere on Earth almost (but not quite) continually since the Neoarchean.
2. The oldest postulated, although controversial, passive margin in the compilation is Steep Rock Lake (Superior Province), ca. 3000–2800 Ma. Modern-style passive margins appear to be absent from the rock record before that time, either because they never existed, have been deformed beyond recognition, have been eroded away, or now rest in the deep crust or mantle.
3. Passive margins are unevenly distributed through the latter half of earth history, with peak abundances at ca. 1900–1890, 610–520, and 150–0 Ma and low abundances at ca. 1740–1000 and 300–275 Ma.
4. The distribution of passive margins through time correlates with parts of the proposed supercontinent cycle, but not with others. Good correlations are seen with the assembly of Nuna, the breakup of Rodinia, and the assembly and breakup of Pangea. The passive-margin record is not obviously consistent with the proposed breakup of Nuna, the assembly of Rodinia, or the assembly or breakup of the putative Pannotia. An alternative scheme is proposed in which Rodinia formed by collision of at least two supercratons, which each had existed through the Mesoproterozoic.
5. The age distribution of passive margins appears to be robust as it shows a remarkable match for the continental component of the seawater $^{87}Sr/^{86}Sr$ secular curve.
6. The still unfinished lifespans were determined for all of the modern-day passive margins. These have an aggregate length of 105,000 km, a mean age of 104 m.y., and a maximum age of 180 m.y.
7. Seventy-six ancient margins have a mean lifespan of 178 m.y. and a range of lifespans from 25 to 590 m.y.
8. The mean lifespan of 47 Precambrian margins was 206 m.y., compared to 15 Paleozoic margins that had a mean lifespan of only 137 m.y. The five longest-lived passive margins, all of them Mesoproterozoic, had lifespans exceeding 350 m.y. It is hard to avoid the conclusion that passive margins lasted longer during the Precambrian. This unexpected finding conflicts with the notion espoused by earlier workers that the tempo of plate tectonics was faster in the Precambrian than at present, because the plates were smaller, moved faster, or both. The longevity of Precambrian

[7] The northern Iberian margin thus defies pigeonholing into either a "modern" or an "ancient" passive margin: it originated as a true passive margin, briefly became a convergent margin, and has since been inactive, though not "passive" according to my definition. Thus it is lumped with the "ancient" margins in this paper.

Author's personal copy



passive margins is consistent instead with Korenaga's (2006) recent modeling of mantle evolution, which suggested that plate tectonics was more sluggish in the Precambrian.

9. Passive-margin collisions have produced–or at least preserved–high-pressure, low-temperature metamorphic conditions only since ca. 625 Ma.
10. Additional research is warranted for all margins, but a few are particularly important. Steep Rock Lake (margin A10) and the Belingue greenstone belt (margin A78) may be the world's oldest passive margins, but tectonic interpretations are controversial and age control is inadequate. The longevity of the Mesoproterozoic passive margins of eastern, western, and southern Siberia (margins A38, A56, and A40) and eastern and northern Baltica (margins A24 and A23) needs to be carefully assessed.

## Acknowledgments

This study was preceded by research in the early 1980s by Kevin Burke, Bill Kidd, and Lauren Bradley into the question of whether or not passive margins convert spontaneously to convergent margins. I concur with them: not often. I especially wish to thank Paul Hoffman for sharing his insights on many of the Proterozoic margins, and David Rowley both for ideas about many of the Phanerozoic margins, and for a set of preliminary age picks for the modern passive margins. I have been helped with various age picks and (or) interpretations by Tanya Atwater, Wouter Bleeker, Kevin Burke, Kevin Chamberlain, Bill Collins, John Dewey, Maarten de Wit, Yildirim Dilek, David Evans, Karl Karlstrom, Tim Kusky, Xiang-Zing Li, Jim Pindell, Sergei Pisarevski, Ali Polat, Celal Sengör, and Fred Ziegler. Graham Shields shared a pre-publication plot of the continental component of seawater strontium through time. Many of the start- and end dates were based on geochronology on key units that were sought out by Sam Bowring and his students. Keith Labay provided GIS support. Figs. 8b and 9b were modified from cross-sections by Peter Cawood and Alexander Khudoley. Reviews by Tim Kusky, Rich Goldfarb, Kent Condie, and Paul Hoffman substantially improved the manuscript. Suggestions and information on additional margins will be gladly received.

## Appendix A. Supplementary data

Supplementary data associated with this article can be found, in the online version, at doi:10.1016/j.earscirev.2008.08.001.

## References

Ashwal, L.D., 1993. Anorthosites. Springer-Verlag, Berlin. 422 pp.
Armstrong, R.A., Compston, W., Retief, E.A., Williams, I.S., Welke, H.J., 1991. Zircon ion microprobe studies bearing on the age and evolution of the Witwatersrand Triad. Precambrian Research 53, 243–266.
Bahlburg, H., Hervé, F., 1997. Geodynamic evolution and tectonostratigraphic terranes of northwestern Argentina and northern Chile. Geological Society of America Bulletin 109, 869–884.
Beukes, N.J., 1984. Sedimentology of the Kuruman and Griquatown iron-formations, Transvaal Supergroup, Griqualand West, South Africa. Precambrian Research 24, 47–84.
Beukes, N.J., 1986. The Transvaal Sequence in Griqualand West. In: Anhaeusser, C.R., Maske, S. (Eds.), Mineral Deposits of South Africa. Geological Society of South Africa, Johannesburg, pp. 819–828.
Bird, J.M., Dewey, J.F., 1970. Lithosphere plate-continental margin tectonics and the evolution of the Appalachian orogen. Geological Society of America Bulletin 81, 1031–1059.
Bleeker, W., 2003. The late Archean record: a puzzle in ca. 35 pieces. Lithos 71, 99–134.
Bond, G.C., Nickeson, P.A., Kominz, M.A., 1984. Breakup of a supercontinent between 625 and 555 Ma: new evidence and implications for continental histories. Earth and Planetary Science Letters 70, 325–345.
Bradley, D.C., 1989. Taconic plate kinematics as revealed by foredeep stratigraphy. Tectonics 8, 1037–1049.
Bradley, D.C., Kidd, W.S.F., 1991. Flexural extension of the upper continental crust in collisional foredeeps. Geological Society of America Bulletin 103, 1416–1438.
Bradley, D.C., Leach, D.L., 2003. Tectonic controls of Mississippi Valley-type lead–zinc mineralization in orogenic forelands. Mineralium Deposita 38, 652–667.
Brookfield, M.E., Hashmat, A., 2001. The geology and petroleum potential of the North Afghan platform and adjacent areas (northern Afghanistan, with parts of southern Turkmenistan, Uzbekistan and Tajikistan). Earth-Science Reviews 55, 41–71.
Burke, K., Dewey, J.F., Kidd, W.S.F., 1976. Dominance of horizontal movements, arc and microcontinental collisions during the later permobile regime. In: Windley, B.F. (Ed.), The Early History of the Earth. John Wiley & Sons, New York, pp. 113–129.
Burke, K., Kidd, W.S.F., Bradley, L.M., 1984. Do Atlantic-type margins convert directly to Andean margins? Geological Society of America Abstracts with Programs, vol. 16, p. 459.
Carter, D.J., Audley-Charles, M.G., Barber, A.J., 1976. Stratigraphical analysis of island arc–continental margin collision in eastern Indonesia. Journal of the Geological Society of London 132, 179–198.
Cawood, P.A., Nemchin, A.A., 2001. Paleogeographic development of the east Laurentian margin: constraints from U–Pb dating of detrital zircons in the Newfoundland Appalachians. Geological Society of America Bulletin 113, 1234–1246.
Cawood, P.A., McCausland, P.J.A., Dunning, G.R., 2001. Opening Iapetus: constraints from the Laurentian margin in Newfoundland. Geological Society of America Bulletin 113, 443–453.
Cawood, P.A., Nemchin, A.A., Strachan, R., 2007A. Provenance record of Laurentian passive-margin strata in the northern Caledonides; implications for paleodrainage and paleogeography. Geological Society of America Bulletin 119, 993–1003.
Commission de la Carte Géologique du Monde, 2000. Carte Géologique du Monde á 1:25,000,000. UNESCO (on CD).
Condie, K.C., 2002. The supercontinent cycle: are there two patterns of cyclicity? Journal of African Earth Sciences 35, 179–183.
Condie, K.C., 2003. Supercontinents, superplumes and continental growth; the Neoproterozoic record. Geological Society Special Publication 206, 1–21.
Condie, K.C., 2005. Earth as an Evolving Planetary System. Elsevier Academic Press, Amsterdam. 447 pp.
Cook, P.J., McElhinny, M.W., 1979. A re-evaluation of the spatial and temporal distribution of sedimentary phosphate deposits in the light of plate tectonics. Economic Geology 74, 315–330.
Cornell, D.H., Armstrong, R.A., Walraven, F., 1998. Geochronology of the Proterozoic Hartley basalt formation, South Africa; constraints on the Kheis tectogenesis and the Kaapvaal Craton's earliest Wilson cycle. Journal of African Earth Sciences 26, 5–27.
Dalziel, I.W.D., 1997. Neoproterozoic–Paleozoic geography and tectonics; review, hypothesis, environmental speculation. Geological Society of America Bulletin 109, 16–42.
Dewey, J.F., Bird, J.M., 1970. Mountain belts and the new global tectonics. Journal of Geophysical Research 75, 2625–2647.
Drake, A.A., Jr., Sinha, A.K., Laird, J., Guy, R.E., 1989. The Taconic orogen. In: Hatcher, R.D., Jr., Thomas, W.A., Viele, G.W. (Eds.), The Appalachian–Caledonian Orogen in the United States. Boulder, Colorado, Geological Society of America, The Geology of North America, v. F-2, 101–177.
Gradstein, F.M., Ogg, J.G., 2004. A Geologic Time Scale 2004. Cambridge University Press, Cambridge. 598 pp., 1 plate.
Grotzinger, J.P., Ingersoll, R.V., 1992. Proterozoic sedimentary basins. In: Schopf, J.W., Klein, C. (Eds.), The Proterozoic Biosphere. Cambridge University Press, Cambridge, pp. 47–50.
Halverson, G.P., Dudás, F.O., Maloof, A.C., Bowring, S.A., 2007. Evolution of the $^{87}Sr/^{86}Sr$ composition of Neoproterozoic seawater. Palaeogeography, Palaeoclimatology, Palaeoecology 256, 103–129.
Hamilton, W., 1979. Tectonics of the Indonesian region. U.S. Geological Surey Professional Paper 1078, 345 p., 1 plate, scale 1:5,000,000.
Harding, C.J., 2004. Origin of the Zeekoebaart and Nauga East high-grade iron ore deposits, Northern Cape Province, South Africa. Master's thesis, University of Johannesburg, South Africa. http://etd.uj.ac.za/theses/available/etd-11302004-091145/.
Hargraves, R.B., 1986. Faster spreading or greater ridge length during the Archean? Geology 14, 750–752.
Hiscott, R.N., 1995. Middle Ordovician clastic rocks of the Humber Zone and St. Lawrence Platform. In: Williams, H., (Ed.), Geology of the Appalachian–Caledonian Orogen in Canada and Greenland. Boulder, Colorado, Geological Society of America, The Geology of North America, v. F-1, 87–98.
Hoffman, P.F., 1980. Wopmay orogen: a Wilson cycle of Early Proterozoic age in the northwest of the Canadian shield. Geological Association of Canada Special Publication 20, 523–549.
Hoffman, P.F., 1987. Early Proterozoic foredeeps, foredeep magmatism, and Superior-type iron-formation of the Canadian Shield. American Geophysical Union Geodynamics Series 17, 85–98.
Hoffman, P.F., 1989. Precambrian geology and tectonic history of North America. In: Bally, A., Palmer, A. (Eds.), The Geology of North America, v. A. Geological Society of America, Boulder, Colorado, pp. 447–512.
Hoffman, P.F., 1991A. Did the breakout of Laurentia turn Gondwanaland inside-out? Science 252, 1409–1412.
Hoffman, P.F., 1997. Tectonic genealogy of North America. In: van der Pluijm, B.A., Marshak, S. (Eds.), Earth Structure: an Introduction to Structural Geology and Tectonics. McGraw-Hill, New York, pp. 459–464.
Hoffman, P.F., Bowring, S.A., 1984. Short-lived 1.9 Ga continental margin and its destruction, Wopmay orogen, northwest Canada. Geology 12, 68–72.
Holland, H.D., 2006. The oxygenation of the atmosphere and oceans. Philosophical Transactions of Royal Society B 361, 903–915.
Jahn, B., Caby, R., Monie, P., 2001. The oldest UHP eclogites in the world: age of UHP metamorphism, nature of protoliths, and tectonic implications. Chemical Geology 178, 143–158.

Author's personal copy



Jenner, G.A., Dunning, G.R., Malpas, J., Brown, M., Brace, T., 1991. Bay of Islands and Little Port complexes, revisited: age, geochemical, and isotopic evidence confirm suprasubduction-zone setting. Canadian Journal of Earth Sciences 28, 1635–1652.
Karabinos, P., Samson, S.D., Hepburn, J.C., Stoll, H.M., 1998. Taconian Orogeny in the New England Appalachians and the Shelburne Falls Arc. Geology 26, 215–218.
Karig, D.E., Barber, A.J., Charlton, T.R., Klemperer, S., Hussong, D.M., 1987. Nature and distribution of deformation across the Banda Arc–Australia collision zone at Timor. Geological Society of America Bulletin, 98, 18–32.
Karlstrom, K.E., Ahall, K.-I., Harlan, S.S., Williams, M.L., McClelland, J., Geissman, J.W., 2001. Long-lived (1.8–1.0 Ga) convergent orogen in southern Laurentia, its extensions to Australia and Baltica, and implications for refining Rodinia. Precambrian research 111, 5–30.
Karlstrom, Karl E., Williams, M.L., McClelland, J., Geissman, J.W., Ahall, K.-I., 1999. Refining Rodinia: geologic evidence for the Australia–Western U.S. connection in the Proterozoic. GSA Today 9 (10), 1–7.
Khudoley, A.A., Guriev, G.A., 2003. Influence of syn-sedimentary faults on orogenic structure: examples from the Neoproterozoic–Mesozoic east Siberian passive margin. Tectonophysics 365, 23–43.
Khudoley, A.K., Rainbird, R.H., Stern, R.A., Kropachev, A.P., Heaman, L.M., Zanin, A.M., Podkovyrov, V.N., Belova, V.N., Sukhorukov, V.I., 2001. Sedimentary evolution of the Riphean–Vendian basin of southeastern Siberia; Rodinia and the Mesoproterozoic Earth–ocean system. Precambrian Research 111, 129–163.
Knight, I., James, N.P., Lane, T.E., 1991. The Ordovician St. George unconformity, Northern Appalachians: the relationship of plate convergence at the St. Lawrence Promontory to the Sauk-Tippecanoe sequence boundary. Geological Society of America Bulletin 103, 1200–1225.
Knight, I., James, N.P., Williams, H., 1995. Cambrian–Ordovician carbonate sequence. In: Williams, H., (Ed.), Geology of the Appalachian–Caledonian Orogen in Canada and Greenland. Boulder, Colorado, Geological Society of America, The Geology of North America, v. F-1, 67–87.
Korenaga, J., 2006. Archean geodynamics and thermal evolution of Earth. Archean Geodynamics and Environments, AGU Geophysical Monograph Series 164, 7–32.
Kristoffersen, Y., 1990. Eurasia Basin. In: Grantz, A., Johnson, G.L., Sweeney, J.F. (Eds.), The Arctic Ocean region. Boulder, Colorado, Geological Society of America, The Geology of North America, v. L, 365–378.
Kusky, T.M., Hudleston, P.J., 1999. Growth and demise of an Archean carbonate platform, Steep Rock Lake, Ontario, Canada. Canadian Journal of Earth Sciences 36, 565–584.
Landing, E., Bartowski, K.E., 1996. Oldest shelly fossils from the Taconic Allochthon and late Early Cambrian sea-levels in eastern Laurentia. Journal of Paleontology 70, 741–761.
Leach, D.L., Bradley, D.C., Lewchuck, M., Symonds, D.T.A., Brannon, J., de Marsily, G., 2001. Mississippi Valley-type lead–zinc deposits through geological time: implications from recent age-dating research. Mineralium Deposita 36, 711–740.
Lister, G.S., Etheridge, M.A., Symonds, P.A., 1991. Detachment models for the formation of passive continental margins. Tectonics 10, 1038–1064.
Longley, I.M., Buessenschuett, C., Clydsdale, L., Cubitt, C.J., Davis, R.C., Johnson, M.K., Marshall, N.M., Murray, A.P., Somerville, R., Spry, T.B., Thompson, N.B., 2002. The North West Shelf of Australia—a Woodside perspective. In: Keep, M., Moss, S. (Eds.), The Sedimentary Basins of Western Australia, 3. Petroleum Exploration Society of Australia, Perth, pp. 27–88.
Malavieille, J., Lallemand, S.E., Dominguez, S., Deschamps, A., Lu, C.-Y., Liu, C.-S., Schnürle, P., 2002. Arc–continent collision in Taiwan: New marine observations and tectonic evolution. In: Byrne, T.B., Liu, S.-C. (Eds.), Geology and Geophysics of an Arc–Continent Collision, Taiwan, Republic of China. Boulder, Colordao, Geological Society of America Special Paper, vol. 358, pp. 187–211.
Mann, P., Gahagan, L., Gordon, M.B., 2003. Tectonic setting of the world's giant oil and gas fields. AAPG Memoir 78, 15–105.
Martin, D.M., Powell, C.M., George, A.D., 2000. Stratigraphic architecture and evolution of the early Paleoproterozoic McGrath Trough, Western Australia. Precambrian Research 99, 33–64.
Maruyama, S., Liou, J.G., Terabayashi, M., 1996. Blueschists and eclogites of the world and their exhumation. International Geology Review 36, 485–594.
Nelson, J., Paradis, S., Christiansen, J., Gabites, J., 2002. Canadian Cordilleran Mississippi Valley-type deposits: a case for Devonian–Mississippian back-arc hydrothermal origin. Economic Geology 97, 1013–1036.
Nisbet, E.G., Fowler, C.M.R., 1983. Model for Archean plate tectonics. Geology, 11, 376–379.
Parfenov, L.M., 1991. Tectonics of the Verkhoyansk-Kolyma Mesozoides in the context of plate tectonics. Tectonophysics 199, 319–342.
Pelechaty, S.M., 1996. Stratigraphic evidence for the Siberia–Laurentia connection and Early Cambrian rifting. Geology 24, 719–722.
Pelechaty, S.M., Grotzinger, J.P., Kashirtsev, V.A., Zhernovsky, V.P., 1996. Chemostratigraphic and sequence stratigraphic constraints on Vendian–Cambrian basin dynamics, Northeast Siberian craton. Journal of Geology 104, 543–564.
Piper, J.D.A., 2000. The Neoproterozoic supercontinent: Rodinia or Palaeopangea? Earth and Planetary Science Letters 176, 131–146.
Pisarevsky, S.A., Natapov, L.M., 2003. Siberia and Rodinia. Tectonophysics 375, 221–245.
Pollack, H.N., 1997. Thermal characteristics of the Archean. In: De Wit, M.J., Ashwal, L.D. (Eds.), Greenstone Belts. Clarendon Press, Oxford, pp. 223–232.
Rainbird, R.H., Stern, R.A., Khudoley, A.K., Kropachev, A.P., Heaman, L.M., Sukhorukov, V.I., 1998. U–Pb geochronology of Riphean sandstone and gabbro from southeast Siberia and its bearing on the Laurentia–Siberia connection. Earth and Planetary Science Letters 164, 409–420.
Rankin, D.W., Hall, L.M., Drake, A.A. Jr., Goldsmith, R., Ratcliffe, N.M., Stanley, R.S., 1989. Proterozoic evolution of the rifted margin of Laurentia. In: Hatcher, R.D., Jr., Thomas, W.A., and Viele, G.W. (Eds.), The Appalachian–Caledonian Orogen in the United States. Boulder, Colorado, Geological Society of America, The Geology of North America, v. F-2, 10–42.
Read, J.F., 1989. Evolution of Cambro-Ordovician passive margin. In: Hatcher, R.D. Jr., Thomas, W.A., Viele, G.W. (Eds.), The Appalachian–Caledonian Orogen in the United States. Boulder, Colorado, Geological Society of America, The Geology of North America, v. F-2, 42–57.
Richter, F.M., Rowley, D.B., DePaolo, D.J., 1992. Sr isotopic evolution of seawater: the role of tectonics. Earth and Planetary Science Letters 109, 11–23.
Rivers, T., 1997. Lithotectonic elements of the Grenville Province: review and tectonic implications. Precambrian Reseach 86, 117–154.
Roberts, D., Siedlecka, A., Olovyanishnikov, V.G., 2004. Neoproterozoic, passive-margin, sedimentary systems of the Kanin Pennusula, and northern and central Timan, NW Russia. Geological Society of London Memoir 30, 5–17.
Rogers, J.J.W., Santosh, M., 2002. Configuration of Columbia, a Mesoproterozoic supercontinent. Gondwana Research 5, 5–22.
Rogers, J.J.W., Santosh, M., 2003. Supercontinents in Earth history. Gondwana Research 6, 357–368.
Rowley, D.B., Kidd, W.S.F., 1981. Stratigraphic relationships and detrital composition of the medial Ordovician flysch of western New England: implications for the tectonic evolution of the Taconic Orogeny. Journal of Geology 89, 199–218.
Schoonmaker, A., Kidd, W.S.F., Bradley, D.C., 2005. Foreland/forearc collisional mafic and granitoid magmatism caused by lower-plate lithospheric slab-breakoff: the Acadian of Maine, and other orogens. Geology 33, 961–964.
Scotese, C.R., 2004. A continental drift flipbook. Journal of Geology 112, 729–741.
Scrutton, R.A., 1982. Crustal structure and development of sheared passive continental margins. American Geophysical Union Geodynamics Series 6, 133–140.
Sengör, A.M.C., 2004. Ribbon continents: a marginal affair of central importance. Geological Society of America Abstacts with Programs 36 (5), 534.
Sengör, A.M.C., Natalin, B.A., 1996. Paleotectonics of Asia: fragments of a synthesis. In: Yin, A., Harrison, T.M. (Eds.), The Tectonic Evolution of Asia. Cambridge University Press, Cambridge, pp. 486–640.
Sengör, A.M.C., Altiner, D., Cin, A., Ustaömer, T., Hsu, K.J., 1988. Origin and assembly of the Tethyside orogenic collage at the expense of Gondwana Land. Geological Society of London Special Publication 37, 119–181.
Sheikholeslami, M.R., Pique, A., Mobayen, P., Sabzehei, M., Bellon, H., Hashem Emami, M., 2008. Tecton-metamorphic evolution of the Neyriz metamorphic complex, Quir-Kor-Sefid area (Sannandaj-Sirjan Zone, SW Iran). Journal of Asian Earth Sciences 31, 504–521.
Shields, G.A., 2007. A normalised seawater strontium isotope curve: possible implications for Neoproterozoic–Cambrian weathering rates and the further oxygenation of the Earth. eEarth 2, 35–42.
Sinclair, H.D., 1997. Tectonostratigraphic model for underfilled peripheral foreland basins: an Alpine perspective. Geological Society of America Bulletin 109, 324–346.
Stampfli, G., Marcoux, J., Baud, A., 1991. Tethyan margins in space and time. Palaeogeography, Palaeoclimatology, Palaeoecology 87, 373–409.
Stevens, R.K., 1970. Cambro-Ordovician flysch sedimentation and tectonics in western Newfoundland and their possible bearing on a proto-Atlantic. Geological Association of Canada Special Paper 7, 165–178.
Tinker, J., de Wit, M., Grotzinger, J., 2002. Seismic stratigraphic constraints on Neoarchean–Paleoproterozoic evolution of the western margin of the Kaapvaal Craton, South Africa. South African Journal of Geology 105, 107–134.
van Staal, C.R., Dewey, J.F., Mac Niocaill, C., McKerrow, W.S., 1998. The Cambrian–Silurian tectonic evolution of the Northern Appalachians and British Caledonides; history of a complex, west and southwest Pacific-type segment of Iapetus. Geological Society Special Publications 143, 199–242.
Veevers, J.J., Falvey, D.A., Robins, S., 1978. Timor Trough and Australia: facies show topographic wave migrated 80 km during the past 3 m.y. Tectonophysics 45, 217–227.
Veizer, J., McKenzie, F.T., 2003. Evolution of sedimentary rocks. Treatise on Geochemistry 7, 369–407.
Vergés, J., García-Senz, J., 2001. Mesozoic evolution and Cainozoic inversion of the Pyreneean rift. Mémoirs du Museum National d'Histoire Naturelle 186, 187–212.
Waldron, J.W.F., van Staal, C.R., 2001. Taconian orogeny and the accretion of the Dashwoods block: A peri-Laurenitan microcontinent in Iapetus ocean. Geology 29, 811–814.
Williams, H., 1995. Taconic allochthons. In: Williams, H., (Ed.), Geology of the Appalachian–Caledonian Orogen in Canada and Greenland. Boulder, Colorado, Geological Society of America, The Geology of North America, v. F-1, 99–114.
Williams, H., Kumarapeli, P.S., Knight, I., 1995. Upper Precambrian–Lower Cambrian clastic sedimentary and volcanic rocks. In: Williams, H., (Ed.), Geology of the Appalachian–Caledonian Orogen in Canada and Greenland. Boulder, Colorado, Geological Society of America, The Geology of North America, v. F-1, 61–67.
Zagorevski, A., Rogers, N., van Staal, C.R., McNicoll, V., Lissenberg, C.J., Valverde-Vaquero, P., 2006. Lower to Middle Ordovician evolution of peri-Laurentian arc and backarc complexes in Iapetus: constraints from the Annieopsquotch accretionary tract, central Newfoundland. Geological Society of America Bulletin 118, 324–342.
Zhao, G., Cawood, P.A., Wilde, S.A., Sun, M., 2002. Review of global 2.1–1.8 Ga orogens: implications for a pre-Rodinia supercontinent. Earth Science Reviews 59, 125–162.
Zhao, G., Sun, M., Wilde, S.A., Sanzhong, L., 2004. A Paleo-Mesoproterozoic supercontinent; assembly, growth and breakup. Earth-Science Reviews 67, 91–123.